**TITLE:**

# Circulating myeloid cell-derived extracellular vesicles as mediators of indirect acute lung injury

Ying Ying Tan[1], Kieran P. O'Dea[1*], Diianeira Maria Tsiridou[1], Aurelie Pac Soo[1], Marissa W. Koh[1], Florence Beckett[1], Masao Takata[1].

[1]Division of Anaesthetics, Pain Medicine & Intensive Care, Imperial College London, Chelsea & Westminster Hospital, 369 Fulham Road, London, UK.

*Corresponding author: Dr Kieran O'Dea, PhD

Division of Anaesthetics, Pain Medicine & Intensive Care, Imperial College London, Chelsea & Westminster Hospital, 369 Fulham Road, London, UK.

k.odea@imperial.ac.uk

Tel.: (+)44 (0)203 315 8292

**Author contribution:** YY.T. and K.P.O. conceived and designed the work, performed experiments, analyzed the data, and prepared the manuscript. DM.T. conceived and designed the work, performed experiments, and analyzed the data A.PS, M.W.K, and F.B performed experiments. M.T. conceived and designed the work, and prepared the manuscript. All authors approved the final version.

**Running Title:** Myeloid extracellular vesicles in acute lung injury

**Grant and funding information:** This work was supported by the Chelsea and Westminster Health Charity, London, UK under Grant P79524, and the British Journal of Anaesthesia/Royal College of Anaesthetists under Grant P66438.



AJRCMB Articles in Press. Published September 23, 2022 as 10.1165/rcmb.2022-0207OC

This article has an online data supplement, which is accessible from this issue's table of content online at www.atsjournals.org.

AJRCMB Articles in Press. Published September 23, 2022 as 10.1165/rcmb.2022-0207OC

## ABSTRACT

Blood-borne myeloid cells, neutrophils and monocytes, play a central role in the development of indirect acute lung injury (ALI) during sepsis and non-infectious systemic inflammatory response syndrome (SIRS). By contrast, the contribution of circulating myeloid cell-derived extracellular vesicles (EVs) to ALI is unknown, despite acute increases in their numbers during sepsis and SIRS. Here, we investigated the direct role of circulating myeloid-EVs in ALI using a mouse isolated perfused lung system and a human cell coculture model of pulmonary vascular inflammation consisting of lung microvascular endothelial cells and peripheral blood mononuclear cells. Total and immunoaffinity-isolated myeloid (CD11b+) and platelet (CD41+) EVs were prepared from the plasma of i.v. LPS-injected endotoxemic donor mice and transferred directly into recipient lungs. Two-hour perfusion of lungs with unfractionated EVs from a single donor induced pulmonary edema formation and increased perfusate levels of receptor for advanced glycation end products (RAGE), consistent with lung injury. These responses were abolished in the lungs of monocyte-depleted mice. The isolated myeloid- but not platelet-EVs produced a similar injury response and the acute intravascular release of proinflammatory cytokines and endothelial injury markers. In the in vitro human coculture model, human myeloid (CD11b+) but not platelet (CD61+) EVs isolated from LPS-stimulated whole blood induced acute proinflammatory cytokine production and endothelial activation. These findings implicate circulating myeloid-EVs as acute mediators of pulmonary vascular inflammation and edema, suggesting an alternative therapeutic target for attenuation of indirect ALI.


AJRCMB Articles in Press. Published September 23, 2022 as 10.1165/rcmb.2022-0207OC

**KEYWORDS:** Acute lung injury; sepsis; extracellular vesicle; neutrophil; monocyte

AJRCMB Articles in Press. Published September 23, 2022 as 10.1165/rcmb.2022-0207OC

## INTRODUCTION

Acute lung injury (ALI) and its severe clinical presentation, acute respiratory distress syndrome (ARDS), are devastating illnesses in critical care with high morbidity and mortality (1, 2). The recent emergence of COVID-19 has highlighted the crucial importance of ARDS in healthcare as well as its disease heterogeneity, pointing to the need for new and existing treatments to be tailored toward specific pathophysiologies. The 'indirect' form of ALI is caused by extrapulmonary insults during systemic infection (sepsis) and non-infectious systemic inflammatory response syndrome (SIRS) (3) that culminate in pulmonary endothelial injury, vascular congestion and interstitial edema (4, 5). Despite the failure of systemic anti-cytokine therapies, targeted attenuation of the pulmonary vascular processes contributing to ALI remains highly desirable but may require a fundamental redirection of research to develop alternative strategies.

In response to activating stimuli, cells increase their release of membrane encapsulated extracellular vesicles (EVs), either via plasma membrane blebbing to produce 'microvesicles', or via exocytosis to release pre-formed 'exosomes' (6). Possessing an array of effector molecules and specific cell-adhesive properties, EVs represent mobile functional subunits of their parent cells. Within the vasculature, circulating EVs may thus function as biological 'vehicles' by encapsulating mediators for targeted delivery to remote sites of injury or infection without activity loss during transit (7). Promotion of processes such as coagulation and inflammation by different EV subtypes is evidence of their essential roles in maintenance of vascular homeostasis. However, circulating levels of EVs, particularly subtypes derived from neutrophils, monocytes and platelets, are increased several-fold during sepsis or sterile SIRS (8-11) implicating them in the aberrant and dysregulated processes responsible for organ injury. Supporting this contention, challenge of mice with in vitro

AJRCMB Articles in Press. Published September 23, 2022 as 10.1165/rcmb.2022-0207OC

generated erythrocyte- or endothelial cell-EVs has been shown to exacerbate lipopolysaccharide (LPS)-induced systemic inflammation and associated indirect ALI (12-15). In contrast, the role of neutrophil- and monocyte-derived EVs has not been described despite a vast body of experimental evidence implicating their parent myeloid cells as drivers of indirect ALI.

The intravascular activities of circulating EVs are tightly controlled under normal conditions through rapid reticuloendothelial system (RES)-mediated clearance, primarily via macrophage uptake in the liver and spleen (16, 17). However, we recently demonstrated a several-fold enhanced uptake of in vitro generated EVs in the lungs by newly marginated pulmonary intravascular monocytes during low-dose LPS-induced endotoxemia in mice (18). By contrast, uptake by liver Kupffer cells decreased, resulting in an overall redirection of circulating EVs to the lungs. This phenomenon indicates that EV-target cell interactions are substantively enhanced within the pulmonary microvasculature even under conditions of relatively low-grade systemic inflammation.

We hypothesized that uptake of circulating myeloid cell-derived EVs within the pulmonary vasculature contributes directly to the pathogenesis of indirect ALI during acute systemic inflammation. To test this hypothesis, we developed a novel ‘endogenous’ EV challenge model based on direct transfer of circulating EVs from endotoxemic mice to an ex vivo isolated perfused lungs (IPL) system. Using total EVs and immunoaffinity-isolated myeloid-EV and platelet-EV subpopulations, we found significant induction of pulmonary edema and release of inflammatory cytokines and soluble injury markers in IPL, with a specific role for myeloid-EVs. The translational significance of these observations was indicated in an in vitro human cell culture model

AJRCMB Articles in Press. Published September 23, 2022 as 10.1165/rcmb.2022-0207OC

of endotoxemia-induced pulmonary microvascular inflammation. Some results of these studies have been previously reported in the form of an abstract (19, 20).

## METHODS

More detailed methods are provided in an online supplement.

### Mouse model of endotoxemia

All protocols were performed in accordance with the Animals (Scientific Procedures) Act 1986, UK. Male C57BL/6 mice (22–26 g; Charles River Laboratories, Margate, UK) were injected i.v. with LPS (2 µg; Ultrapure *Escherichia coli* O111:B4; InvivoGen, Toulouse, France) to produce an acute endotoxemia with mild clinical symptoms (21). Heparinized blood was collected at 1, 2 or 4 h, and platelet-poor plasma (PPP) obtained for EV analysis by flow cytometry. Circulating EV recoveries were enhanced using the clodronate-liposome method of macrophage depletion to reduce EV clearance (18, 22, 23). Clodronate-liposomes were injected i.v. (0.2 ml) followed by i.v. LPS challenge after 48 h when vascular Ly6C$^{high}$ monocytes but not Ly6C$^{low}$ monocytes, liver and splenic macrophages are replenished (Supplementary Figure 2)(18, 21).

### Human whole blood model of EV production

Blood collection from healthy volunteer donors was approved by a local research ethics committee. Heparinized blood was incubated with LPS (100 ng/ml) with continuous mixing for 1 - 4 h. PPP was prepared for EV analysis by flow cytometry and EV subtype isolation.

AJRCMB Articles in Press. Published September 23, 2022 as 10.1165/rcmb.2022-0207OC

## EV quantification

EV subtypes were identified and quantified by flow cytometry, as described previously (10, 18).

## EV subtype isolation

EV-enriched suspensions were prepared from mouse and human PPP by centrifugation at 20,800 × *g* for 30 min at 4°C, washed and resuspended in PBS-BSA. Subtype counts were determined by flow cytometry and then incubated with MACS® MicroBeads (~50 nm diameter, Miltenyi Biotec, Bisley, UK) at a ratio of 1 µl bead suspension to 1 × $10^6$ target EVs for 30 min at 4°C. EV-bead suspensions were then applied to magnetized LS columns (Miltenyi Biotec) and washed with three 3 ml flushes of PBS-BSA. Column-bound EVs were eluted in 3 ml of PBS-BSA, centrifuged at 20,800 × *g* for 30 min at 4°C and resuspended in IPL perfusion buffer or tissue culture media.

## IPL model of ALI

We used a mouse IPL model system (18, 24) to determine the direct contribution of circulating EVs to ALI excluding systemic cellular or humoral responses. Prior to IPL, mice were injected with a low-dose of LPS (i.v., 20 ng) to induce conditions of enhanced circulating EV uptake within the pulmonary vasculature (18). EVs were infused into the IPL and recirculated under closed circuit conditions for 2 h. Lung injury was assessed by wet-to-dry weight (W/D) ratio and bronchoalveolar lavage fluid

AJRCMB Articles in Press. Published September 23, 2022 as 10.1165/rcmb.2022-0207OC

(BALF) protein concentration (24). Perfusate cytokines and soluble injury markers were measured by ELISA.

**Human model of pulmonary vasculature inflammation**

Isolated EV subtypes were incubated in co-cultures of primary human lung microvascular endothelial cells (HLMECs) and peripheral blood mononuclear cells (PBMCs) from healthy volunteer donors for 4 h. Cell adhesion molecule expression on HLMEC was assessed by flow cytometry and cytokine levels by ELISA.

**Statistics**

Group comparisons were made using Student's t-tests, ANOVA with Bonferroni tests or Kruskal-Wallis with Dunn's tests. Data are presented as mean±SD or median with interquartile ranges (median±IQR). Statistical significance was defined as $p < 0.05$.

AJRCMB Articles in Press. Published September 23, 2022 as 10.1165/rcmb.2022-0207OC

## RESULTS

### *Increases in neutrophil- and monocyte-derived EVs during acute endotoxemia*

To investigate the acute changes in levels of circulating EV subtypes during endotoxemia, mice were injected with a single bolus i.v. LPS dose of 2 μg which we previously found to produce significant inflammation but only minor visible clinical effects (21, 25). Among the vascular cell-derived EV subtypes analysed in PPP, there was a rapid and marked elevation of two distinct CD11b+ EV subtypes displaying either Ly6C+, Ly6G+ or Ly6C+, Ly6G- phenotypes, consistent with neutrophil and Ly6C$^{high}$ monocyte cell origins, respectively (Supplementary Figure 1). By 1 h after LPS injection, these neutrophil- and Ly6C$^{high}$ monocyte-EV subtypes increased from relatively low baseline levels by ~100-fold and ~10-fold, respectively, and remained significantly elevated up to the final 4 h time point (**Figure 1**). In contrast, EVs derived from platelets (CD41+), endothelial cells (CD31+, CD41-) and erythrocytes (TER-119+) were much higher at baseline but remained unchanged. Circulating macrophage-derived EVs were also investigated on the basis of their F4/80 marker expression (26), but they were not detectable in control or LPS-challenged mice.

### *Enhancement of circulating EV levels by pre-depletion of intravascular macrophages*

Circulating EVs are rapidly cleared from the circulation, primarily through their uptake by resident intravascular macrophages of the liver and spleen RES (17, 27). To evaluate the total release of EVs into the circulation during endotoxemia, we pre-treated mice with i.v. clodronate-liposomes to deplete intravascular macrophages 48 h prior to LPS challenge and thereby reduce endogenous EV clearance. At this time-

AJRCMB Articles in Press. Published September 23, 2022 as 10.1165/rcmb.2022-0207OC

point after clodronate pre-treatment, circulating Ly6C$^{high}$ monocytes are replenished from the bone marrow (18, 21)(Supplementary Figure 2). At 1 h post-LPS, numbers of all circulating EV subtypes were found to be ≥10-fold higher than in non-clodronate liposome pre-treated mice (**Figure 2**), consistent with previous studies assessing intravascular trafficking of EVs (18, 22, 23).

### *Circulating EVs from endotoxemic mice induce indirect ALI*

We implemented the RES inhibition method in adoptive transfer donor mice to enable recovery of EVs more representative of the total intravascular EV output during endotoxemia and substantially reduce numbers of donor mice required. The recipient IPL was prepared from a mouse that had been in vivo 'primed' for 2 h with low-dose LPS (i.v. 20 ng), to simulate conditions of enhanced EV uptake by the lungs (18). Washed EVs (~1.0 × $10^8$) from a single i.v. LPS (1 h) treated donor mouse were then infused into the perfusion circuit in serum-free buffer, and the IPL was run in a recirculating manner for 2 h. IPL challenge with the in vivo derived EVs induced a significant increase in lung W/D ratio, substantive increases in perfusate levels of the lung injury marker, receptor for advanced glycation end products (RAGE), but no change in BALF protein concentration, indicative of an interstitial edema (**Figure 3**). To assess the involvement of intravascular monocytes in EV-mediated pulmonary edema and injury, recipient mice were pre-treated i.v. with clodronate-liposomes 24 h prior to the in vivo LPS priming step before monocyte repopulation from the bone marrow has occurred (21, 24)(Supplementary Figure 3). We found that near complete reversal of the EV-induced increases in W/D ratio and RAGE resulted, indicating a critical role for lung-marginated monocytes in EV-induced lung injury (Figure 3).

AJRCMB Articles in Press. Published September 23, 2022 as 10.1165/rcmb.2022-0207OC

***Myeloid-EVs induce indirect ALI and release of pro-inflammatory cytokines***

To define these injury-promoting activities of total EVs and the contribution of neutrophil (Ly6C+, Ly6G+) and monocyte (Ly6C+, Ly6G-) derived myeloid-EVs, we developed an immunoaffinity isolation-based methodology. Platelet-EVs were also investigated as a comparator control population of similar abundance in vivo. EVs from two RES-inhibited LPS-treated (1 h) donor mice were subjected to positive immunoaffinity bead-based selection (Supplementary Figure 4) using anti-CD11b to enrich for myeloid-EVs or anti-CD41 for platelet-EVs. A standardized dose of $9.0 \times 10^7$ EVs, based on the mean numbers of circulating myeloid-EVs (CD11b+, Ly6C+) per ml of plasma, were infused directly into the IPL from a low-dose LPS-pretreated recipient mouse and recirculated for 2 h. Myeloid-EVs caused significant increases in lung W/D ratio (**Figure 4**) compared to control untreated IPL and to the platelet EV-treated IPL. Compared to control IPL, platelet-EVs produced a statistically significant but much lower W/D ratio increase. Myeloid-EVs, but not platelet-EVs, induced significant increases in levels of perfusate RAGE. Taken together, these data suggest that myeloid EVs are responsible in large part for injury responses produced by total EVs.

Concentrations of inflammatory and vascular injury-related markers were measured in perfusates harvested at the end of 2 h IPL procedure. Myeloid-EVs induced significant increases in levels of key pro-inflammatory cytokines and chemokines (TNF-$\alpha$, IL-6, KC, MIP-1$\alpha$, MIP-2, MCP-1, RANTES, and GM-CSF) as well as soluble markers of endothelial injury (endothelin-1 (ET-1), angiotensin converting enzyme (ACE), angiopoietin-2 (Angpt-2) and vascular endothelial growth factor (VEGF)) (**Table 1**). In sharp contrast to myeloid-EVs, platelet-EVs had no

AJRCMB Articles in Press. Published September 23, 2022 as 10.1165/rcmb.2022-0207OC

discernible effect on soluble mediator levels, except for a significant increase in Angpt-2, at similar levels to myeloid-EVs. Therefore, endogenous myeloid-EVs are potent inducers of acute pro-inflammatory soluble mediator release, as well as of endothelial activation and injury marker release from within the pulmonary vasculature.

***Activity of whole blood derived EV subtypes in a human model of pulmonary vascular inflammation***

To explore the translational potential of the mouse EV-induced pulmonary injury/inflammation findings, EV subtypes were isolated from a whole blood model of sepsis-related inflammation and assayed for their pro-inflammatory activity in a human *in vitro* model of pulmonary vascular inflammation. Healthy volunteer blood was stimulated with LPS (100 ng/ml) *ex vivo* to produce EVs containing mixed subtypes. CD66b+ neutrophil-EVs levels were increased significantly, reaching a maximum at 3 h post-LPS stimulation, whereas CD14+ monocyte-EVs did not increase from baseline. In contrast, platelet-EV (CD41+, CD61+) levels peaked earlier and were higher throughout the time course (**Figure 5**). These lower levels of human myeloid subtypes in vitro differed substantially those in LPS-challenged mice, where circulating myeloid- and platelet-EVs reached similar levels.

Myeloid-EVs (CD11b+ EVs) and platelet-EVs (CD61+ EVs) were isolated from fresh PPP by positive immunoaffinity bead-based selection (Supplementary Figure 6). EV subtypes were incubated with HLMECs alone or in coculture with PBMCs standardized to $6 \times 10^6$ EVs/well based on our previous observation of maximum neutrophil CD66b+ EVs numbers in 1 ml of sepsis patient plasma (10). In coculture, myeloid-EVs induced upregulation of ICAM-1, VCAM-1 and E-selectin expression on

AJRCMB Articles in Press. Published September 23, 2022 as 10.1165/rcmb.2022-0207OC

HLMEC and significant release of pro-inflammatory cytokines (TNF-$\alpha$, IL-8 and MCP-1) (**Figure 6**). Platelet-EVs induced only a small increase in VCAM-1 expression and no significant pro-inflammatory cytokine release. Neither EV subtype had any effect on cell adhesion molecule expression or pro-inflammatory cytokine release (Supplementary Figure 7) in HLMEC monoculture, indicating the EV-induced responses were PBMC-dependent. Overall, these results closely resemble the mouse *ex vivo* IPL findings, suggesting that myeloid-EVs would have potent pro-inflammatory activity within the human pulmonary vasculature.

***Uptake of EVs from isolated neutrophils in PBMC-HLMEC coculture***

Finally, to address potential influence of bead binding on EV-target cell interactions in our models, we compared the uptake and bioactivity of 'bead-bound' vs 'untouched' EVs in the in vitro model of pulmonary microvascular inflammation. A pure single subpopulation of myeloid-EVs derived from isolated human neutrophils was used for this purpose: neutrophils were isolated from volunteer blood, labeled with the lipophilic fluorescent dye DiD, and stimulated with N-formylmethionine-leucyl-phenylalanine (fMLP). The DID-labeled EVs (Supplementary Figure 8) were incubated either alone or with anti-CD11b beads followed by centrifugation, and these 'untouched' or 'bead-bound' DID-labelled neutrophil EVs were then added to the PBMC-HLMEC coculture for 1h. We found that substantive levels of DiD fluorescence were associated with monocytes, HLMEC and B cells (CD11b-, CD19+), but very low levels in the remaining CD11b-, CD19-, predominantly T cell population (**Figure 7** and Supplementary Figure 8). Preincubation of neutrophil-EVs with beads increased their uptake by monocytes and to a lesser degree, by HLMEC and B cells. However, these neutrophil EVs, either

AJRCMB Articles in Press. Published September 23, 2022 as 10.1165/rcmb.2022-0207OC

untouched or bead-bound, did not produce inflammatory responses in our coculture model, suggesting that binding of anti-CD11b beads to EVs could promote their uptake but would not *per se* generate significant inflammatory response in target cells.

AJRCMB Articles in Press. Published September 23, 2022 as 10.1165/rcmb.2022-0207OC

## DISCUSSION

Despite increased levels of circulating myeloid-EVs being frequently observed in sepsis and SIRS patients, their direct pulmonary-specific effects and contribution to indirect ALI are not known. Here, we investigated the contribution of in vivo generated myeloid-EVs to indirect ALI during endotoxemia in mice, using IPL as the established model of choice for evaluating 'direct' relationships between circulating mediators and pulmonary vascular inflammation/injury. By using this novel in vivo-to-ex vivo adoptive transfer approach, we obtained the first definitive evidence that systemically released myeloid-EVs are direct mediators of pulmonary vascular inflammation/injury.

We first investigated the early kinetics of circulating EV subtypes following LPS challenge to gauge pulmonary vascular exposure to EVs produced during acute episodes of systemic inflammation. Of the EV subtypes analyzed, only neutrophil- and Ly6C$^{high}$ subset monocyte-derived EVs showed acute substantive increases from their relatively low baselines, indicating increased exposure of cells within the pulmonary vasculature to these subsets during an endotoxemia. Single injection LPS-induced endotoxemia, rather than live bacterial challenge, is an ideal sepsis/SIRS model for precise measurements of such acute response kinetics and avoids the inevitable contamination of in vivo derived preparations with bacteria or their EVs (28). Previous animal and human volunteer studies of circulating EVs have mainly focused on their pro-coagulant activity (29-32) with limited analysis of individual subtype levels, but in line with our findings, early sampling (i.e. within 24 h of ICU admission) of human sepsis, meningitis and severe burn injury patients has demonstrated acute increases in circulating EV subtypes, particularly granulocyte, platelet- and monocyte-derived (9-11).



AJRCMB Articles in Press. Published September 23, 2022 as 10.1165/rcmb.2022-0207OC

We evaluated intravascular macrophage depletion as a novel strategy to enhance circulating EV levels and hence their recovery for the direct in vivo EV to ex vivo IPL challenge studies. Due to rapid intravascular clearance, mainly by the RES, circulating levels of EVs represent only the net balance between production and clearance (23). Suppressing RES clearance by intravascular macrophage depletion has been used as an effective tool for elucidating intravascular trafficking of injected EVs (18, 22, 23). Using macrophage depletion in normal mice, Matsumoto et al. calculated a circulating half-life of ~7 minutes for injected exosomes and an ~3-fold increase in levels of circulating endogenous EVs (23). Similarly, we found enhanced levels of all endogenous EV subtypes in LPS-challenged mice, ≥10-fold higher compared to macrophage intact mice. Consequently, it was possible to use only one or two donor mice macrophage-depleted donor mice, as opposed to 10-20 intact mice, to generate physiologically relevant quantities of circulating myeloid EVs for IPL challenge experiments. Such rapid clearance of EVs can be inferred in humans by the increases in circulating EVs produced by cardiac stress returning to normal levels after 1 h (33) and higher levels in splenectomized individuals (34). Therefore, as proposed for circulating cytokines (35), circulating EVs represent only a ‘tip of the iceberg’ or temporal snapshot of total systemic EV output and biological function.

Using EVs from a single macrophage-depleted mouse donor in a two-hour IPL challenge protocol, we sought to determine the cumulative impacts of EVs released during an acute episode of endotoxemia. The outcome was a consistent pattern of increased lung W/D ratio and perfusate RAGE, but no change in BALF protein, indicating the development of interstitial edema. We then addressed the role of individual EV subtypes, but in contrast to conventional analysis of 'in vitro' generated EVs from single parent cells in response to a single cell-specific agonist stimulation in

AJRCMB Articles in Press. Published September 23, 2022 as 10.1165/rcmb.2022-0207OC

cell culture, we used 'in vivo' generated, immunoaffinity-isolated EV subtypes. We reasoned that by generation of EVs in vivo and immunoaffinity selection of subtypes, direct and meaningful comparisons between different EV subtypes released under the identical SIRS condition can be achieved. We found that challenge with isolated myeloid-EVs but not platelet-EVs, produced the same pattern of injury as total unfractionated EVs, demonstrating subtype specificity, and at the same time ruling out artefacts such as vascular injury from particulate infusion or non-specific carry over of soluble mediators such as LPS and cytokines from mouse plasma. These conclusions were reinforced by the potent induction of cytokines and pulmonary endothelial cell activation by myeloid- but not platelet-EVs in both the mouse IPL and human coculture assay.

Several studies have shown that systemic injection of in vitro-generated EVs (endothelial- and erythrocyte-derived) can enhance or potentiate LPS-induced ALI in mice (12-14). In contrast to our ex vivo IPL-based evaluation of indirect ALI mechanisms, in vivo systemic EV challenge does not distinguish between their local pulmonary-specific and systemic extra-pulmonary effects. Mechanistic insights into systemic EV-enhanced ALI have been obtained by Zecher et al., showing that erythrocyte-EV injection triggers thrombin-mediated increases in plasma C5a levels and C5a-receptor-dependent pro-inflammatory cytokine production (12). Since prothrombotic activity is common to different vascular EV subtypes (8, 9), these findings suggest a generalized mechanism by which bolus administration of any EV subtype can promote immuno-thrombotic processes within circulating blood with potential to further exacerbate organ injury. However, we deliberately avoided such ‘systemic’ humoral responses in our IPL and in vitro coculture systems by use of a plasma/serum-free buffering system. Instead, our models assessed the direct

AJRCMB Articles in Press. Published September 23, 2022 as 10.1165/rcmb.2022-0207OC

pulmonary-specific responses generated by interactions between specific EV subtypes (i.e. myeloid- and platelet-EVs) and their target cells (e.g. lung-marginated monocytes and endothelial cells) within the pulmonary microvasculature.

Development of monocyte-dependent injury in the mouse IPL and PBMC-dependent pro-inflammatory responses in the coculture model suggest an essential role for monocytes as mediators of myeloid-EV induced indirect ALI during endotoxemia. A recent study by Danesh et al. comparing the inflammatory properties of EVs released spontaneously from isolated vascular cell populations, demonstrated that neutrophil- and monocyte-EVs induce pro-inflammatory cytokine release from monocytes after 24 h incubations, whereas platelet-EVs were largely inactive inducing only the anti-inflammatory cytokine TGF-β (36). Here, the rapid and potent production of inflammatory mediators in the IPL and coculture suggest a mechanism by which myeloid-EV stimulated monocytes could orchestrate pulmonary vascular inflammation *in situ*. By contrast, several studies have linked neutrophil-EVs to anti-inflammatory responses and processes (15), including suppression of pro-inflammatory responses in human monocyte-derived macrophages via Mer tyrosine kinase (MerTK) receptor signalling (36, 37), a cell surface receptor for membrane phosphatidylserine that is absent from undifferentiated monocytes (38). Based on our previous demonstration of increased monocyte uptake of circulating EVs during endotoxemia (18), a dichotomy may therefore exist in which opposing or differential responses of monocytes and macrophages to myeloid-EVs play a critical role in regulating tissue-specific inflammation during sepsis/SIRS. However, despite several published studies demonstrating uptake of circulating EVs by liver and splenic macrophages in vivo, their responses to myeloid-EVs have, to our knowledge, not been reported.

AJRCMB Articles in Press. Published September 23, 2022 as 10.1165/rcmb.2022-0207OC

The direct contribution of myeloid-EVs to pulmonary vascular inflammation and edema is in line with the critical roles of this lineage of cells in ALI, and as such, certain effects previously ascribed to their parent cell effector molecules may instead be derived from their EVs. For example, neutrophil elastase and myeloperoxidase are present in active forms on EV surfaces (39, 40), suggesting that circulating EV capture by the lungs would focus such pro-injurious activities directly onto the pulmonary endothelium. Moreover, myeloid-EVs may be more potent long-range mediators of injury than their parent cell-derived soluble mediators, which are neutralized by endogenous antagonists within blood (35, 41). As such, our findings contribute to an alternative paradigm of indirect ALI in sepsis and SIRS, where EVs dominate over secreted pro-inflammatory mediators as circulating endocrine mediators of their parent cell effector functions.

Our use of physiologically relevant models of EV production demonstrated pulmonary-specific effects of myeloid-EV subtypes produced during endotoxemia but also created some experimental uncertainties. Although the total EV preparations induced lung edema and RAGE increases in the IPL model, positive immunomagnetic bead separation of EV subtypes had the potential to modify the responses investigated. Indeed, we found that the anti-CD11b beads enhanced the uptake of EVs from fMLP-stimulated isolated neutrophils by monocytes in the in vitro PBMC-HLMEC coculture model. However, these EVs were inactive and, as with platelet-EVs, their association with beads failed to generate pro-inflammatory responses. Thus, although beads enhanced EV-monocyte interactions, they were not themselves capable of generating pro-inflammatory responses, either alone, or bound to EVs.

There were substantial differences between the production of blood EV subtypes in the in vivo mouse and ex vivo human model systems. Both the amount

AJRCMB Articles in Press. Published September 23, 2022 as 10.1165/rcmb.2022-0207OC

and rate of LPS-induced myeloid-EV release in the whole blood model were substantially lower than in mice. In sepsis patients, circulating neutrophil-EVs can reach levels similar to platelets-EVs (9, 11), while monocyte-EVs levels are substantially lower than neutrophil-EVs, consistent with the relative abundance of their parent cells. We observed a similar pattern in mice, with neutrophil-EVs levels similar to platelet-EVs, and monocyte-EVs increased but to a lesser degree. However, in the human whole blood model, LPS-induced neutrophil-EV release was delayed and substantially lower than in mice, while monocyte-EV numbers did not appear to increase at all. The higher myeloid-EV levels in vivo may reflect the additional cell sources, including the non-circulating marginated pools and the bone marrow and splenic reservoirs that are rapidly mobilized into the blood during inflammation (21, 42). However, the more rapid increases observed in mice and lack of monocyte-EVs in the human whole blood model, suggest that other local and systemic factors contribute to circulating EV release during endotoxemia. Clearly, these in vivo and in vitro model-related differences in EV production deserve further exploration, but also point to the need for functional studies on individual circulating EV subtypes isolated from LPS-challenged human volunteers or sepsis/SIRS patients.

In conclusion, our findings suggest that investigating the vascular bed-specific interactions and functions of EVs is requisite to defining their biological roles and clinical significance. We have shown that with a relatively brief exposure to physiologically relevant quantities of circulating myeloid-EVs, there is a substantive pulmonary vascular response of acute inflammation and increased permeability, hallmarks of the early stages of indirect ALI. Given the recurrent nature of endotoxemia in sepsis patients (43), reducing such circulating myeloid-EV-pulmonary vascular interactions could therefore be an effective vascular-bed specific strategy for

AJRCMB Articles in Press. Published September 23, 2022 as 10.1165/rcmb.2022-0207OC

attenuating ALI, with clear advantages over the current single mediator-targeted systemic anti-inflammation approaches.

AJRCMB Articles in Press. Published September 23, 2022 as 10.1165/rcmb.2022-0207OC

## ACKNOWLEDGEMENTS

None

## REFERENCES

1. Bellani G, Laffey JG, Pham T, Fan E, Brochard L, Esteban A, Gattinoni L, van Haren F, Larsson A, McAuley DF, et al. Epidemiology, patterns of care, and mortality for patients with acute respiratory distress syndrome in intensive care units in 50 countries. *JAMA* 2016;315(8):788-800.

2. Matthay MA, Ware LB, Zimmerman GA. The acute respiratory distress syndrome. *J Clin Invest* 2012;122(8):2731-2740.

3. Shaver CM, Bastarache JA. Clinical and biological heterogeneity in acute respiratory distress syndrome: Direct versus indirect lung injury. *Clin Chest Med* 2014;35(4):639-653.

4. Pelosi P, D'Onofrio D, Chiumello D, Paolo S, Chiara G, Capelozzi VL, Barbas CSV, Chiaranda M, Gattinoni L. Pulmonary and extrapulmonary acute respiratory distress syndrome are different. European Respiratory Society;2003. p. 48s-56s.

5. Rocco PRM, Pelosi P. Pulmonary and extrapulmonary acute respiratory distress syndrome: Myth or reality? : Curr Opin Crit Care;2008. p. 50-55.

6. Yanez-Mo M, Siljander PR, Andreu Z, Zavec AB, Borras FE, Buzas EI, Buzas K, Casal E, Cappello F, Carvalho J, et al. Biological properties of extracellular vesicles and their physiological functions. *J Extracell Vesicles* 2015;4:27066.

AJRCMB Articles in Press. Published September 23, 2022 as 10.1165/rcmb.2022-0207OC

7. Loyer X, Vion AC, Tedgui A, Boulanger CM. Microvesicles as cell-cell messengers in cardiovascular diseases. *Circ Res* 2014;114(2):345-353.

8. Joop K, Berckmans RJ, Nieuwland R, Berkhout J, Romijn FP, Hack CE, Sturk A. Microparticles from patients with multiple organ dysfunction syndrome and sepsis support coagulation through multiple mechanisms. *Thromb Haemost* 2001;85(5):810-820.

9. Nieuwland R, Berckmans RJ, McGregor S, Boing AN, Romijn FP, Westendorp RG, Hack CE, Sturk A. Cellular origin and procoagulant properties of microparticles in meningococcal sepsis. *Blood* 2000;95(3):930-935.

10. O'Dea KP, Porter JR, Tirlapur N, Katbeh U, Singh S, Handy JM, Takata M. Circulating microvesicles are elevated acutely following major burns injury and associated with clinical severity. *PLoS One* 2016;11(12):e0167801.

11. Lashin HMS, Nadkarni S, Oggero S, Jones HR, Knight JC, Hinds CJ, Perretti M. Microvesicle subsets in sepsis due to community acquired pneumonia compared to faecal peritonitis. *Shock* 2018;49(4):393-401.

12. Zecher D, Cumpelik A, Schifferli JA. Erythrocyte-derived microvesicles amplify systemic inflammation by thrombin-dependent activation of complement. *Arterioscler Thromb Vasc Biol* 2014;34(2):313-320.

13. Belizaire RM, Prakash PS, Richter JR, Robinson BR, Edwards MJ, Caldwell CC, Lentsch AB, Pritts TA. Microparticles from stored red blood cells activate neutrophils and cause lung injury after hemorrhage and resuscitation. *J Am Coll Surg* 2012;214(4):648-655; discussion 656-647.

AJRCMB Articles in Press. Published September 23, 2022 as 10.1165/rcmb.2022-0207OC

14. Buesing KL, Densmore JC, Kaul S, Pritchard KA, Jr., Jarzembowski JA, Gourlay DM, Oldham KT. Endothelial microparticles induce inflammation in acute lung injury. *J Surg Res* 2011;166(1):32-39.

15. Mahida RY, Matsumoto S, Matthay MA. Extracellular vesicles: A new frontier for research in acute respiratory distress syndrome. *Am J Respir Cell Mol Biol* 2020;63(1):15-24.

16. Al Faraj A, Gazeau F, Wilhelm C, Devue C, Guerin CL, Pechoux C, Paradis V, Clement O, Boulanger CM, Rautou PE. Endothelial cell-derived microparticles loaded with iron oxide nanoparticles: Feasibility of MR imaging monitoring in mice. *Radiology* 2012;263(1):169-178.

17. Willekens FL, Werre JM, Kruijt JK, Roerdinkholder-Stoelwinder B, Groenen-Dopp YA, van den Bos AG, Bosman GJ, van Berkel TJ. Liver Kupffer cells rapidly remove red blood cell-derived vesicles from the circulation by scavenger receptors. *Blood* 2005;105(5):2141-2145.

18. O'Dea KP, Tan YY, Shah S, B VP, K CT, Wilson MR, Soni S, Takata M. Monocytes mediate homing of circulating microvesicles to the pulmonary vasculature during low-grade systemic inflammation. *J Extracell Vesicles* 2020;9(1):1706708.

19. Tan YY, O'Dea KP, Takata M. Circulating neutrophil-derived microvesicles during endotoxaemia induce pulmonary vascular injury. *American Journal of Respiratory and Critical Care Medicine* 2020;201.

20. Tsiridou DM, O'Dea KP, Tan YY, Takata M. Late breaking abstract - myeloid-derived microvesicles as acute mediators of sepsis-induced lung vascular inflammation. *European Respiratory Journal* 2020;56.

AJRCMB Articles in Press. Published September 23, 2022 as 10.1165/rcmb.2022-0207OC

21. O'Dea KP, Wilson MR, Dokpesi JO, Wakabayashi K, Tatton L, van Rooijen N, Takata M. Mobilization and margination of bone marrow Gr-1$^{high}$ monocytes during subclinical endotoxemia predisposes the lungs toward acute injury. *Journal of immunology (Baltimore, Md : 1950)* 2009;182(2):1155-1166.

22. Imai T, Takahashi Y, Nishikawa M, Kato K, Morishita M, Yamashita T, Matsumoto A, Charoenviriyakul C, Takakura Y. Macrophage-dependent clearance of systemically administered b16bl6-derived exosomes from the blood circulation in mice. *J Extracell Vesicles* 2015;4:26238.

23. Matsumoto A, Takahashi Y, Chang HY, Wu YW, Yamamoto A, Ishihama Y, Takakura Y. Blood concentrations of small extracellular vesicles are determined by a balance between abundant secretion and rapid clearance. *J Extracell Vesicles* 2020;9(1):1696517.

24. Tatham KC, O'Dea KP, Romano R, Donaldson HE, Wakabayashi K, Patel BV, Thakuria L, Simon AR, Sarathchandra P, Harefield Pi, et al. Intravascular donor monocytes play a central role in lung transplant ischaemia-reperfusion injury. *Thorax* 2018;73(4):350-360.

25. O'Dea KP, Young AJ, Yamamoto H, Robotham JL, Brennan FM, Takata M. Lung-marginated monocytes modulate pulmonary microvascular injury during early endotoxemia. *Am J Respir Crit Care Med* 2005;172(9):1119-1127.

26. Teoh NC, Ajamieh H, Wong HJ, Croft K, Mori T, Allison AC, Farrell GC. Microparticles mediate hepatic ischemia-reperfusion injury and are the targets of diannexin (asp8597). *PLoS One* 2014;9(9):e104376.

27. Wiklander OP, Nordin JZ, O'Loughlin A, Gustafsson Y, Corso G, Mager I, Vader P, Lee Y, Sork H, Seow Y, et al. Extracellular vesicle in vivo biodistribution is

AJRCMB Articles in Press. Published September 23, 2022 as 10.1165/rcmb.2022-0207OC

determined by cell source, route of administration and targeting. *J Extracell Vesicles* 2015;4:26316.

28. Liu A, Park JH, Zhang X, Sugita S, Naito Y, Lee JH, Kato H, Hao Q, Matthay MA, Lee JW. Therapeutic effects of hyaluronic acid in bacterial pneumonia in ex vivo perfused human lungs. *Am J Respir Crit Care Med* 2019;200(10):1234-1245.

29. Aras O, Shet A, Bach RR, Hysjulien JL, Slungaard A, Hebbel RP, Escolar G, Jilma B, Key NS. Induction of microparticle- and cell-associated intravascular tissue factor in human endotoxemia. *Blood* 2004;103(12):4545-4553.

30. Zubairova LD, Zubairov DM, Andrushko IA, Svintenok GY, Mustafin IG. Cell microvesicles during experimental endotoxemia. *Bull Exp Biol Med* 2006;142(5):573-576.

31. Wang JG, Manly D, Kirchhofer D, Pawlinski R, Mackman N. Levels of microparticle tissue factor activity correlate with coagulation activation in endotoxemic mice. *J Thromb Haemost* 2009;7(7):1092-1098.

32. Mooberry MJ, Bradford R, Hobl EL, Lin FC, Jilma B, Key NS. Procoagulant microparticles promote coagulation in a factor XI-dependent manner in human endotoxemia. *J Thromb Haemost* 2016;14(5):1031-1042.

33. Augustine D, Ayers LV, Lima E, Newton L, Lewandowski AJ, Davis EF, Ferry B, Leeson P. Dynamic release and clearance of circulating microparticles during cardiac stress. *Circ Res* 2014;114(1):109-113.

34. Fontana V, Jy W, Ahn ER, Dudkiewicz P, Horstman LL, Duncan R, Ahn YS. Increased procoagulant cell-derived microparticles (C-MP) in splenectomized patients with ITP. *Thromb Res* 2008;122(5):599-603.

AJRCMB Articles in Press. Published September 23, 2022 as 10.1165/rcmb.2022-0207OC

35. Cavaillon JM, Munoz C, Fitting C, Misset B, Carlet J. Circulating cytokines: The tip of the iceberg? *Circ Shock* 1992;38(2):145-152.

36. Eken C, Martin PJ, Sadallah S, Treves S, Schaller M, Schifferli JA. Ectosomes released by polymorphonuclear neutrophils induce a MerTK-dependent anti-inflammatory pathway in macrophages. *J Biol Chem* 2010;285(51):39914-39921.

37. Gasser O, Schifferli JA. Activated polymorphonuclear neutrophils disseminate anti-inflammatory microparticles by ectocytosis. *Blood* 2004;104(8):2543-2548.

38. Zizzo G, Hilliard BA, Monestier M, Cohen PL. Efficient clearance of early apoptotic cells by human macrophages requires M2C polarization and MerTK induction. *Journal of immunology (Baltimore, Md : 1950)* 2012;189(7):3508-3520.

39. Genschmer KR, Russell DW, Lal C, Szul T, Bratcher PE, Noerager BD, Abdul Roda M, Xu X, Rezonzew G, Viera L, et al. Activated PMN exosomes: Pathogenic entities causing matrix destruction and disease in the lung. *Cell* 2019;176(1-2):113-126 e115.

40. Slater TW, Finkielsztein A, Mascarenhas LA, Mehl LC, Butin-Israeli V, Sumagin R. Neutrophil microparticles deliver active myeloperoxidase to injured mucosa to inhibit epithelial wound healing. *Journal of immunology (Baltimore, Md : 1950)* 2017;198(7):2886-2897.

41. Goldie AS, Fearon KC, Ross JA, Barclay GR, Jackson RE, Grant IS, Ramsay G, Blyth AS, Howie JC. Natural cytokine antagonists and endogenous antiendotoxin core antibodies in sepsis syndrome. The sepsis intervention group. *JAMA* 1995;274(2):172-177.

AJRCMB Articles in Press. Published September 23, 2022 as 10.1165/rcmb.2022-0207OC

42. Swirski FK, Nahrendorf M, Etzrodt M, Wildgruber M, Cortez-Retamozo V, Panizzi P, Figueiredo JL, Kohler RH, Chudnovskiy A, Waterman P, et al. Identification of splenic reservoir monocytes and their deployment to inflammatory sites. *Science (New York, NY)* 2009;325(5940):612-616.

43. Klein DJ, Derzko A, Foster D, Seely AJ, Brunet F, Romaschin AD, Marshall JC. Daily variation in endotoxin levels is associated with increased organ failure in critically ill patients. *Shock* 2007;28(5):524-529.

AJRCMB Articles in Press. Published September 23, 2022 as 10.1165/rcmb.2022-0207OC

**Table 1**: Levels of soluble cytokines and endothelial markers in perfusates after IPL with myeloid- and platelet-EVs

| Analyte | Concentration (pg/ml) | | |
|---|---|---|---|
| | **Untreated** | **CD11b+ EVs** | **CD41+ EVs** |
| **ACE** | 41,431±7,404 | 59,006±13,613* | 34,278±4,227 |
| **Angpt-2** | 4,252±469 | 6,241±1,240** | 6,074±593** |
| **ET-1** | 0.13±0.08 | 0.33±0.14* | 0.21±0.13 |
| **GM-CSF** | 3±2 | 19±10*** | 6±5 |
| **IL-1β** | 3±4 | 6±3 | 6±5 |
| **IL-10** | 63±25 | 56±18 | 68±17 |
| **IL-6** | 731±480 | 2,309±261*** | 1,308±737 |
| **KC** | 475±195 | 1,505±535*** | 281±142 |
| **MCP-1** | 165±43 | 271±33** | 162±65 |
| **MIP-1α** | 80±58 | 1,044±187**** | 102±68 |
| **MIP-2** | 422±610 | 1,852±980** | 72±13 |
| **RANTES** | 616±295 | 1,449±200** | 974±382 |
| **TNF-α** | 39±37 | 1,856±1,081*** | 165±273 |
| **VEGF** | 14±4 | 18±2# | 12±3 |

Mean ± SD. *p<0.05, **p<0.01, ***p<0.001 vs. untreated control; #p<0.05 vs. platelet-EVs. n=6-7.

AJRCMB Articles in Press. Published September 23, 2022 as 10.1165/rcmb.2022-0207OC

## FIGURE LEGENDS

**Figure 1 Circulating EV subtype levels during acute endotoxemia.** Mice were injected i.v. with LPS (2 μg) and circulating EV subtype counts in platelet poor plasma (PPP) were determined by flow cytometry. Significant increases were observed in circulating levels of CD11b+, Ly6G+ neutrophil-EVs (◯) and CD11b+, Ly6G-, Ly6C+ monocyte-EVs (□) in PPP at 1 h post-LPS, remaining elevated up to the final 4 h time-point. No change in the levels of platelet-EVs (△), endothelial-EVs (◇), and erythrocyte-EVs (⬡) were observed. Data are log-transformed, displayed as mean ± SD and analysed by one-way ANOVA with Bonferroni's correction tests. $n$ = 4-6, *$p$ < 0.05, **$p$ < 0.01.

**Figure 2. Depletion of intravascular macrophages increases circulating EV subtypes levels during endotoxemia**. Mice were injected with clodronate-liposomes ("clod") (i.v., 0.2 ml). At 48 h, when Ly6C$^{high}$ monocytes, but not macrophages or Ly6C$^{low}$ monocytes, were repopulated from bone marrow, mice were injected i.v. with LPS (2 μg). Circulating levels of CD11b+, Ly6G+ neutrophil-EVs (◯), CD11b+, Ly6G-, Ly6C+ monocyte-EVs (□), platelet-EVs (△), endothelial-EVs (◇), and erythrocyte-EVs (⬡) in PPP at 1 h post-LPS injection were determined by flow cytometry. All EV subtypes were increased as a result of macrophage depletion suggesting reduced clearance. Data are log-transformed, displayed as mean ± SD and analysed by *t*-tests. $n$ = 4-6, **$p$ < 0.01, ***$p$ < 0.001.

**Figure 3. Circulating EVs from endotoxemic mice induce monocyte-dependent lung injury.** Circulating EVs were prepared from clodronate-liposome (0.2 ml, i.v.,

AJRCMB Articles in Press. Published September 23, 2022 as 10.1165/rcmb.2022-0207OC

48 h) and LPS (2 μg, i.v., 1 h) treated mice by differential centrifugation. Washed EVs from a single donor mouse (~1.0 × $10^8$ EVs) were then infused directly into a recipient mouse IPL and recirculated for 2 h. Lung injury was assessed by tissue wet-to-dry weight (W/D) ratios (A), BALF protein concentration (B), and perfusate RAGE concentration (C). In some recipient IPL mice, clodronate-liposomes were injected (i.v., 0.2 ml) 26 h before IPL ('IPL-clod') to deplete pulmonary intravascular monocytes. Data are displayed as mean ± SD and analysed by one-way ANOVA with Bonferroni's correction tests. $n$ = 5-7, *$p$ < 0.05, ****$p$ < 0.001.

**Figure 4. Circulating myeloid-EVs from endotoxemic mice induce lung injury.** Circulating CD11b+ myeloid and CD41+ platelet EV subtypes were isolated from clodronate-liposome (0.2 ml, i.v., 48 h) and LPS (2 μg, i.v., 1 h) treated mice by immunomagnetic bead selection. Washed EVs (9.0 × $10^7$) were then infused directly into a recipient mouse IPL and recirculated for 2 h. Lung injury was assessed by tissue wet-to-dry weight (W/D) ratios (A), BALF protein concentration (B), and perfusate RAGE concentration (C). Data are displayed as mean ± SD and analysed by one-way ANOVA with Bonferroni's correction tests. $n$ = 5-7, *$p$ < 0.05, ****$p$ < 0.001.

**Figure 5. EV subtype levels in LPS-treated blood from healthy volunteers.** Heparinized blood from healthy volunteers was stimulated with LPS (100ng/ml) with continuous mixing for 1-4 h at 37°C. Levels of neutrophil-EVs (◯),monocyte-EVs (□), platelet-EVs (△) and erythrocyte-EVs (⎔) in PPP were determined by flow cytometry. Data are log-transformed, displayed as mean ± SD and analysed by one-

AJRCMB Articles in Press. Published September 23, 2022 as 10.1165/rcmb.2022-0207OC

way ANOVA with Bonferroni's correction tests. $n = 3$, *$p < 0.05$, **$p < 0.01$, ***$p < 0.001$.

**Figure 6. Pro-inflammatory activity of myeloid-EVs from LPS-treated healthy volunteer blood.** CD11b+ myeloid and CD61+ platelet EV subtypes were isolated by immunomagnetic bead selection from LPS (100ng/ml) treated healthy volunteer blood at 3 h. Washed EVs ($6 \times 10^6$) were then incubated with PBMC-HLMECs co-cultures for 4 h. Treatment with myeloid-EVs induced significant increases in expression (MFI: mean fluorescence intensity) of cell adhesion molecules (A) ICAM-1, (B), VCAM-1 and (C) E-selectin in HLMECs and the release of (D) TNF-$\alpha$, (E) IL-8 and (F) MCP-1 into cell culture supernatants. Data are analysed by one-way ANOVA with Bonferroni's correction tests (A and B; mean ± SD) or Kruskal-Wallis with Dunn's tests (C, D, E and F; median ± interquartile range). n = 4-7, * $p<0.05$, **$p < 0.01$, ***$p < 0.001$, **** $p<0.0001$.

**Figure 7. Uptake and activity of EVs released from isolated neutrophils in PBMC-HLMEC coculture.** DiD-labeled or unlabeled neutrophils isolated from healthy volunteer blood were stimulated with fMLP (1 μM) for 30 min to produce EVs. EVs were then pre-incubated alone or with anti-CD11b beads, washed by centrifugation. DiD labelled EVs (25,000 fluorescent units/ml) were then added to PBMC-HLMECs co-cultures and incubated for 1 h. Levels of cell-associated DiD fluorescence are shown for monocytes (CD11b+, CD14+) (A) and HLMECs (CD146+) (B). After 4 h incubation, neither untouched nor bead-bound EVs produced measurable increases in expression (MFI: mean fluorescence intensity) of ICAM-1

AJRCMB Articles in Press. Published September 23, 2022 as 10.1165/rcmb.2022-0207OC

on HLMECs (C) , or release of TNF-$\alpha$ into cell culture supernatants (D). Data are analysed by one-way ANOVA with Bonferroni's correction tests (A, B and C; mean ± SD) or Kruskal-Wallis with Dunn's tests (D; median ± interquartile range). n = 4, $^{**}p < 0.01$, $^{***}p < 0.001$.

AJRCMB Articles in Press. Published September 23, 2022 as 10.1165/rcmb.2022-0207OC

Figure 1

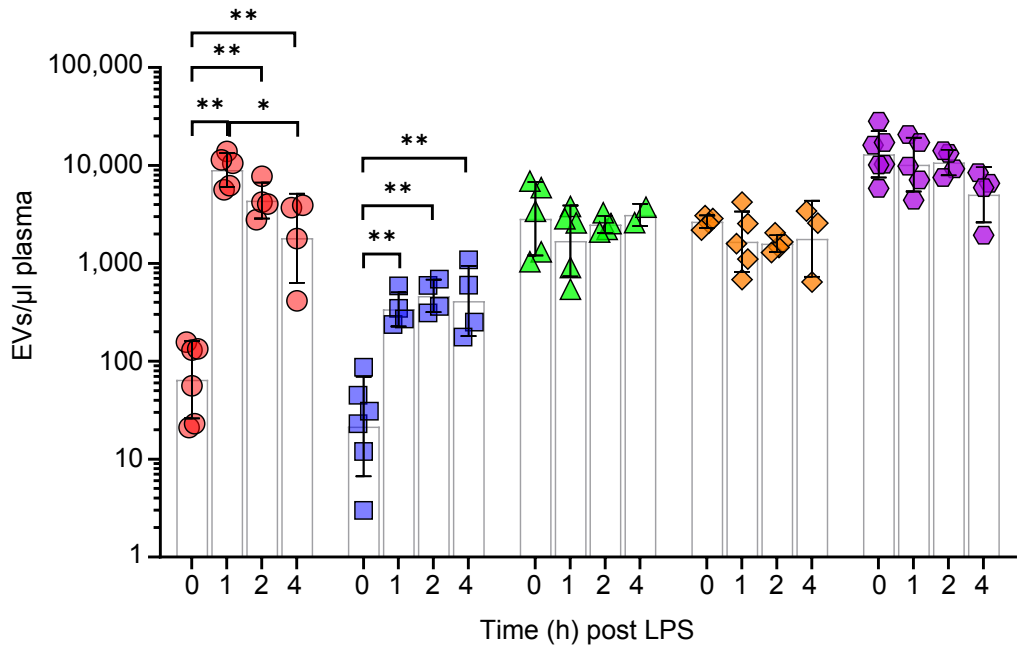


AJRCMB Articles in Press. Published September 23, 2022 as 10.1165/rcmb.2022-0207OC

Figure 2

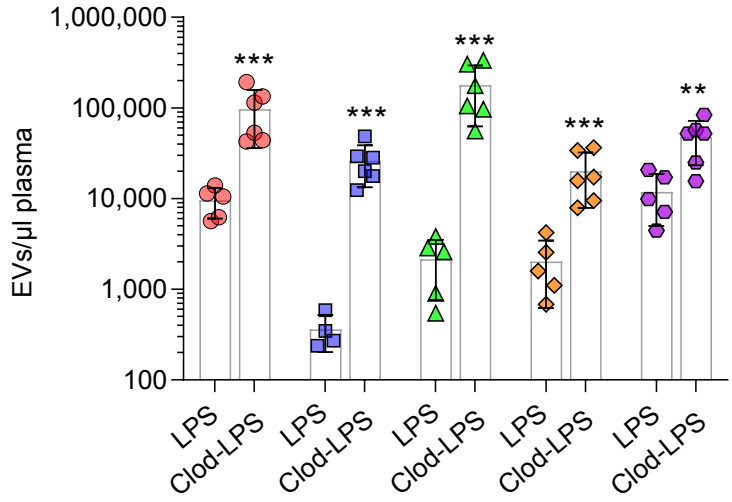


AJRCMB Articles in Press. Published September 23, 2022 as 10.1165/rcmb.2022-0207OC

Figure 3

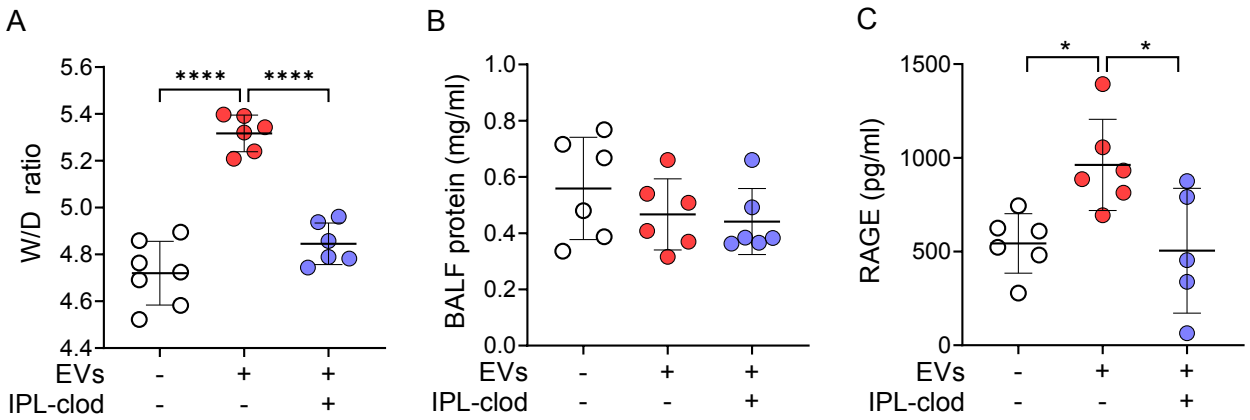


AJRCMB Articles in Press. Published September 23, 2022 as 10.1165/rcmb.2022-0207OC

Figure 4

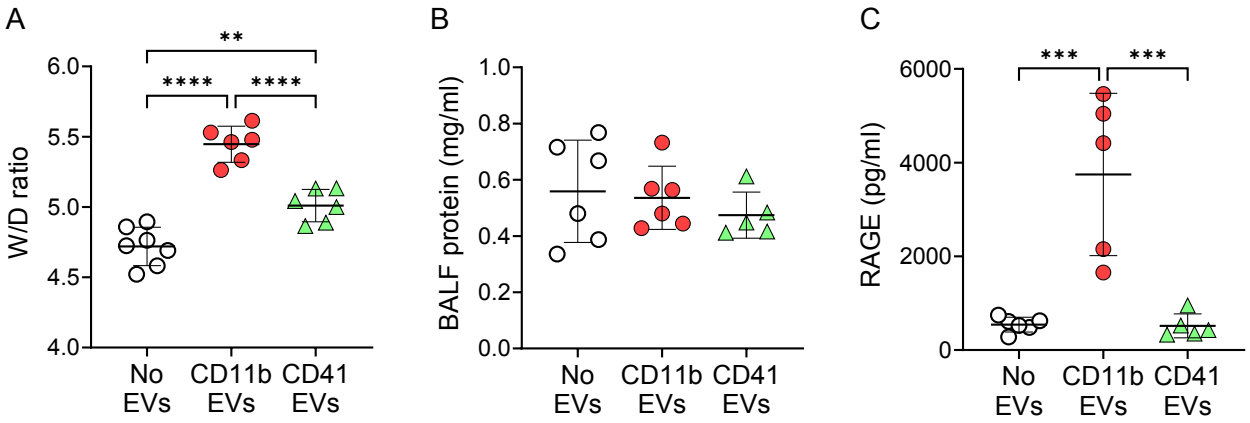


AJRCMB Articles in Press. Published September 23, 2022 as 10.1165/rcmb.2022-0207OC

Figure 5

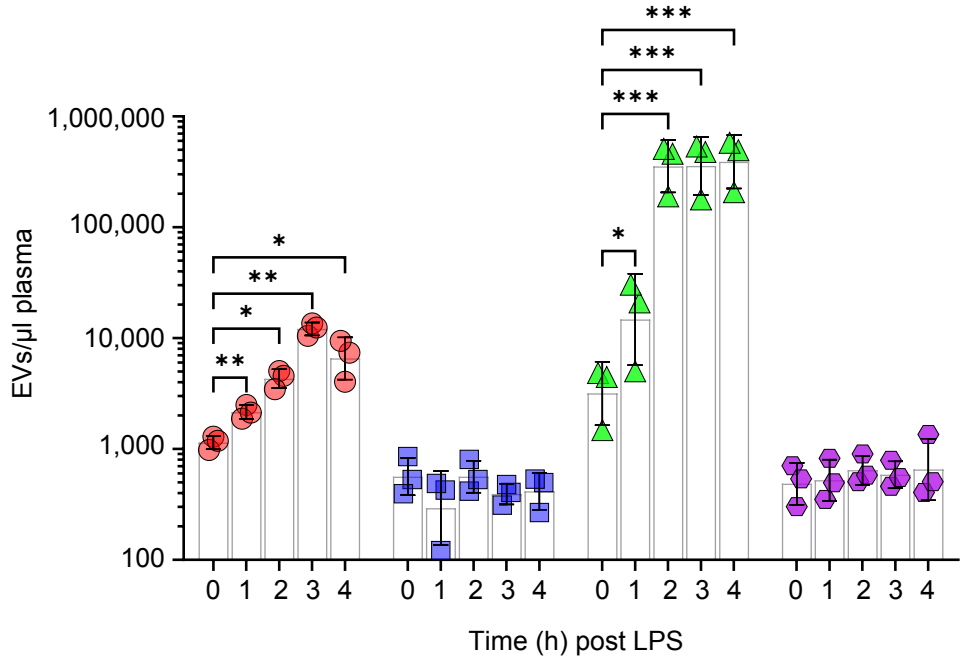


AJRCMB Articles in Press. Published September 23, 2022 as 10.1165/rcmb.2022-0207OC

Figure 6

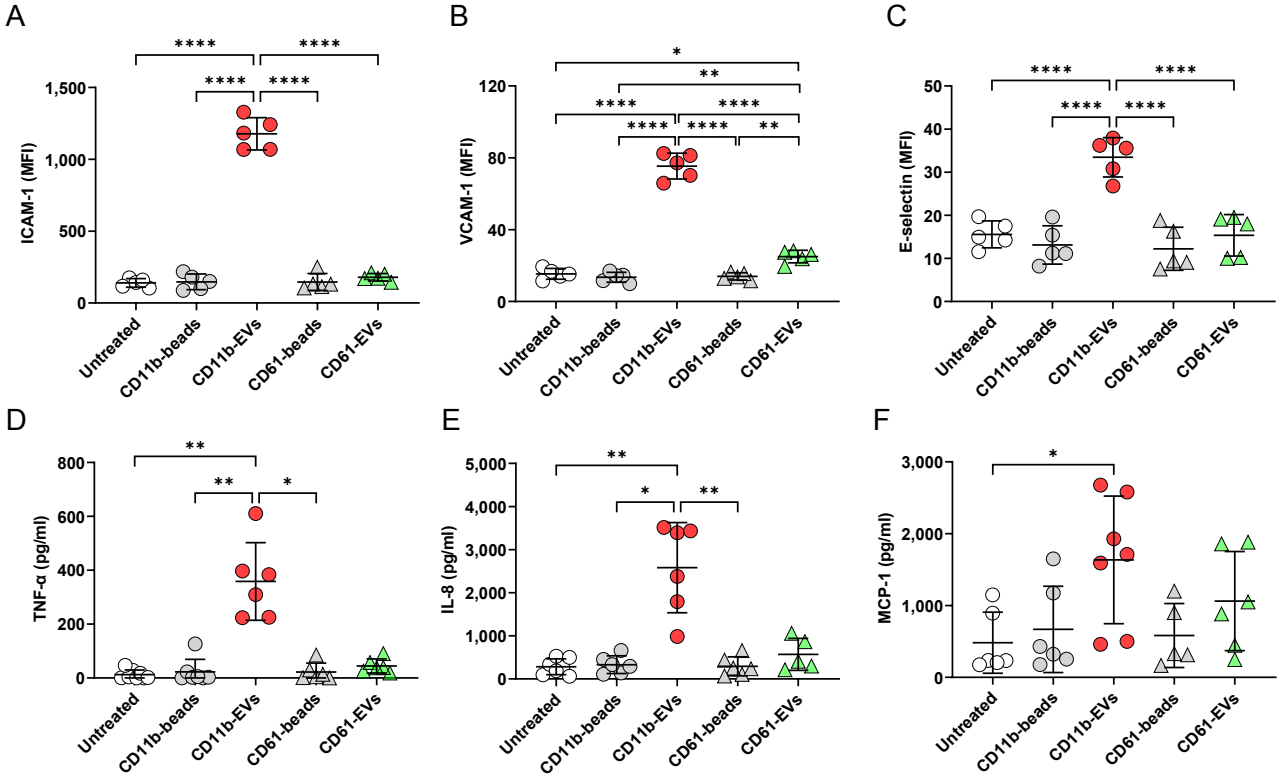


AJRCMB Articles in Press. Published September 23, 2022 as 10.1165/rcmb.2022-0207OC

Figure 7

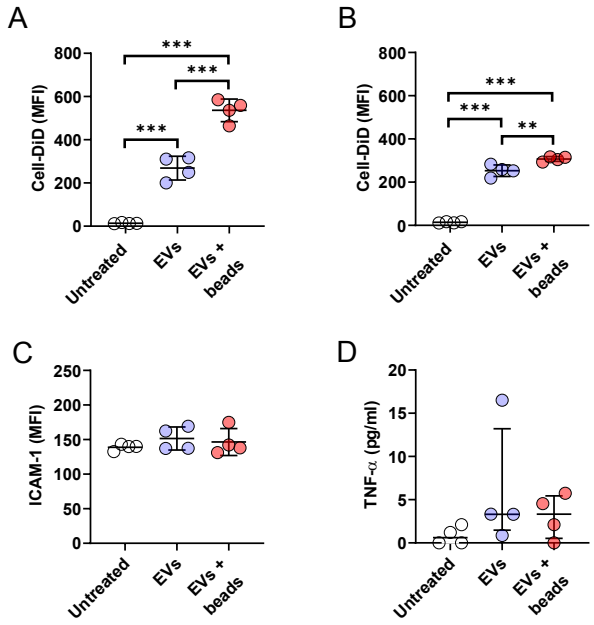


AJRCMB Articles in Press. Published September 23, 2022 as 10.1165/rcmb.2022-0207OC

# Circulating myeloid cell-derived extracellular vesicles as mediators of indirect acute lung injury

Ying Ying Tan, Kieran P. O'Dea, Diianeira Maria Tsiridou, Aurelie Pac Soo, Marissa W. Koh, Florence Beckett, Masao Takata

## ONLINE DATA SUPPLEMENT



AJRCMB Articles in Press. Published September 23, 2022 as 10.1165/rcmb.2022-0207OC

### *Animal husbandry*

All protocols were reviewed and approved by the UK Home Office in accordance with the Animals (Scientific Procedures) Act 1986, UK. Male C57BL/6 mice (Charles River Laboratories, Margate, UK) ages 10–12 weeks (22–26 g) were used (n = 66 in total) for all protocols.

### *In vivo mouse model of endotoxemia and EV production*

Mice were injected intravenously (i.v.) via tail vein with moderate-dose LPS (2 μg in 0.2 ml PBS; Ultrapure *Escherichia coli* O111:B4; InvivoGen, Toulouse, France) to produce an acute endotoxemia but with relatively mild clinical symptoms, as described previously (1). At set time points (1, 2 or 4 h) after LPS challenge, mice were anaesthetized with intraperitoneal (i.p.) xylazine (13 mg/kg) & ketamine (130 mg/kg). Abdominal laparotomy was conducted to expose inferior vena cava for injection of 20 UI heparin in 0.2 ml saline. After 1 min the animal was terminated by exsanguination withdrawing 1 ml of the venous blood into a syringe via a 23G needle. The blood was centrifuged immediately in an Eppendorf angle rotor (FA45-30-11) microfuge at 1,000 × *g* for 10 min at 4°C to sediment cells and the plasma supernatant centrifuged at 1,000 × *g* for a further 5 min at 4°C to obtain platelet-poor plasma (PPP). EVs were isolated by sedimentation at 20,800 × *g* for 30 min at 4°C, washed and resuspended in serum-free IPL perfusion buffer (see below) for total EV challenge, or in PBS, 0.5% tissue-culture grade sterile BSA (Sigma, Poole, UK) prior to immunomagnetic bead separation of EV subtypes.

### *Macrophage depletion in vivo*



AJRCMB Articles in Press. Published September 23, 2022 as 10.1165/rcmb.2022-0207OC

To enhance EV recovery for ex vivo challenge experiments, we investigated the clodronate-liposome method of macrophage depletion to reduce circulating EV clearance (2-4). Clodronate-liposomes (0.2 ml, Formumax Scientific, Palo Alto, California, USA) were injected i.v. and LPS challenge (2 µg) was performed after 48 h when vascular Ly6C$^{high}$ monocytes are replenished, but before significant restoration of blood Ly6C$^{low}$ monocytes (1, 5, 6), or liver and splenic macrophages (7, 8). To assess the role of intravascular lung-marginated monocytes in IPL responses to infused EVs, clodronate-liposomes were injected 26 h prior to IPL before replenishment of Ly6C$^{high}$ and Ly6C$^{low}$ monocytes had taken place (1, 9).

***Ex vivo human whole blood model of EV production***

Blood collection from healthy volunteer donors was approved by a local research ethics committee (NRES Committee London - Camden & Islington, reference 15/LO/1764). Venipuncture was performed into heparinized vacutainers and transferred to 15 ml conical tubes and incubated with LPS (100 ng/ml) at 37°C for 1-4 h with continuous mixing. Cells were then pelleted by centrifugation at 1,000 × *g* for 10 min at 4°C in a swing-out rotor and the plasma supernatant centrifuged at 1,500 × *g* for a further 15 min at 4°C in an Eppendorf angle rotor (FA45-30-11) to obtain PPP. EVs were isolated by centrifugation at 20,800 × *g* for 30 min at 4°C, washed and resuspended in PBS-BSA prior to immunomagnetic bead separation of EV subtypes.

***Immunoaffinity isolation of EV subtypes***

Mouse and human EV subtypes were isolated using an immunomagnetic bead separation method. EV suspensions in PBS-BSA were analyzed by flow cytometry to determine subtype counts and then incubated with MACS® MicroBeads (~50 nm



AJRCMB Articles in Press. Published September 23, 2022 as 10.1165/rcmb.2022-0207OC

diameter, Miltenyi Biotec, Bisley, UK) at a ratio of 1 µl bead suspension to 1 × $10^6$ target EVs for 30 min at 4°C. Anti-CD11b conjugated beads were used for human and mouse myeloid-EVs, anti-CD61 conjugated for human platelet-EVs. For mouse platelet-EV isolation it was necessary to perform an indirect bead-binding method, incubating EV suspensions with biotinylated anti-CD41 (Miltenyi Biotec) followed by anti-biotin immunomagnetic beads (Miltenyi Biotec). EV-bead suspensions were loaded onto magnetized LS columns (Miltenyi Biotec) which were then washed exhaustively by 3 × 3 ml PBS-BSA flushes. Following magnet removal, column-bound EVs were eluted in 3 ml PBS-BSA, centrifuged at 20,800 × *g* for 30 min at 4°C and resuspended in IPL perfusion buffer or tissue culture media for subsequent studies.

***Generation and fluorescence labeling of EVs from isolated neutrophils***

Neutrophils were isolated from healthy volunteer donor blood using the two layer Histopaque 1077 and 1119 (Sigma) density gradient centrifugation method (10). The neutrophil layer was collected and erythrocytes lysed with water. After washing, neutrophils were suspended in RPMI-1640 with 0.5% BSA and 0.5 ml added per 1.5 ml Eppendorf tube and then stimulated with fMLP (1 µM) at 37ºC for 30 min on a rotating wheel. Cells were removed by centrifugation at 800 × *g* for 10 mins at 4ºC followed by centrifugation of supernatants at 20,800 × *g* for 30 mins to pellet EVs. For production of fluorescently labeled EVs, we followed our previous method (4) using the fluorescent membrane dye 1,1′-dioctadecyl-3,3′,3′-tetramethylindodicarbocyanine (DiD, ThermoFisher Scientific, UK), but to avoid sedimentation of insoluble DiD aggregates during centrifugation of directly labeled EVs, neutrophils were labeled prior to EV production. DiD was diluted in Diluent C (Sigma) and incubated at a final concentration of 5 µM with neutrophils (5 × $10^6$/ ml) suspended in PBS (without calcium



AJRCMB Articles in Press. Published September 23, 2022 as 10.1165/rcmb.2022-0207OC

or magnesium) with 0.1% BSA for 20 mins at room temperature. Following two centrifugation washes at 300 × *g* for 5 mins to remove unincorporated DiD, neutrophils were stimulated with fMLP as above to produce DiD-labelled EVs (Supplementary Figure 8). DiD labeling of EVs was evaluated by flow cytometry and the amount of incorporated DiD fluorescence units (FU/ml) measured in PBS, Triton X-100 (0.5%) at 635 nm/680 nm excitation/emission in a Biotek FLx800 plate reader.

***Isolated perfused lung (IPL) model of ALI***

The direct contribution of EVs to ALI was assessed in a serum-free mouse IPL model system as described previously (4, 9, 11), with only minor modifications. Prior to IPL setup, mice were injected with low-dose LPS (i.v., 20 ng), to induce a subclinical endotoxaemia (1) and recreate the conditions of enhanced EV uptake and cellular interactions within the pulmonary vasculature (4). After 2 h, mice were anesthetized with intraperitoneal (i.p.) xylazine (13 mg/kg) & ketamine (130 mg/kg) and injected i.v. with 20 IU of heparin via a tail vein. Tracheostomy was carried out and lungs were given two sustained inflation breaths (5s, 25cm$H_2O$) and ventilation commenced at a tidal volume of 6-7 ml/kg, at respiratory rate of 80 breaths/min, positive end expiratory pressure (PEEP) of 5 cm-$H_2O$, with 21% $FiO_2$. Abdominal laparotomy was carried out in the IPL chamber and the mouse was then exsanguinated via the IVC. The sub-hepatic portion of lower abdomen was removed, and rinsed with sterile saline. Lungs were maintained at continuous positive airway pressure (CPAP) of 5 cm-$H_2O$ to prevent accidental injury during thoracotomy and ventilation gas switched from 21% $FiO_2$ to 5% $CO_2$/21% $O_2$ to ensure normocapnia. To isolate the lung circulation, the pulmonary artery and left atrium were cannulated, and the pulmonary circulation perfused with RPMI-1640 supplemented with 4% tissue-culture grade BSA perfusion



AJRCMB Articles in Press. Published September 23, 2022 as 10.1165/rcmb.2022-0207OC

buffer with osmolality adjusted to 350mOsmol/kg and pH to 7.4. Following a 15 min stabilizing perfusion at a 25/kg/min flow rate, washed EVs obtained from donor mice were infused into the closed, recirculating circuit. For total EV challenges, ~1.0 × $10^8$ (determined by flow cytometry) EVs obtained from one mouse at 1 h after LPS injection were transferred of which ~50% were CD11b+ myeloid derived. For subtype challenge, we used two donors and 9.0 × $10^7$ myeloid-EVs (CD11b+, Ly6C+) based on the mean levels of this subtype per ml of plasma at 1 h post-LPS injection. The experimental design for adoptive transfer of in vivo generated EVs to ex vivo IPL is summarized in Supplementary Figure 5.

**Sample harvesting and processing**

IPL experiments were terminated after 2 h. Lung injury was assessed by wet-to-dry weight (W/D) ratio and bronchoalveolar lavage fluid (BALF) protein concentration, as previously described (9, 11). The right lower lobe was tied off and removed for W/D ratio determination: wet weight was measured immediately, and dry weight was measured after lung was placed in 65°C oven for 24 h. The remaining lobes were lavaged by flushing and gently aspirating 0.65 ml of saline in and out of the lungs via the endotracheal tube three times. The recovered lavage fluid was centrifuged at 300 × *g* for 5 min at 4°C and the supernatant was collected for determination of protein concentration. Total IPL perfusate (~2.5 ml) was collected and centrifuged at 300 × *g* for 10 min at 4°C followed by 20,800 × *g* for 30 min at 4°C to prepare an EV-free supernatant for measurement of soluble mediators and markers by ELISA.

***In vitro human co-culture model of pulmonary vascular inflammation***



AJRCMB Articles in Press. Published September 23, 2022 as 10.1165/rcmb.2022-0207OC

Primary human lung microvascular endothelial cells (HLMECs, Sigma) were cultured in EGM™-2 MV media (Lonza, Basel, Switzerland) and used between passages 5-8. HLMEC were seeded into 48 well plates overnight at confluence ($6.0 \times 10^4$/well). PBMCs were isolated by Histopaque®-1077 (Sigma) density gradient centrifugation and added to HLMECs in serum-free media (EGM™, Lonza; human serum albumin 0.5%, BioIVT, UK) at a monocyte density of $1.2 \times 10^5$/well. After resting for 2 h, EV subtypes were added to HLMEC-PBMCs co-cultures in a total volume of 0.25 ml and cultured for 4 h. The media was then collected and centrifuged at 300 × *g* to remove cells and a further 20,800 × *g* for 30 min to remove EVs and then frozen for cytokine analysis by ELISA. Adherent cells were detached with cell dissociation buffer (Sigma), centrifuged at 400 x g for 5 min at 4°C, washed and resuspended in flow cytometry buffer ( PBS, 2% fetal bovine serum, 0.1% sodium azide, and 2mM EDTA) before antibody staining.

***Flow cytometry***

Cells were incubated with antibodies diluted in flow cytometry buffer and washed by centrifugation, while EVs were incubated in antibodies diluted in 0.1 μm filtered PBS followed a non-centrifugation wash by further dilution in PBS. Antibody staining was performed at 4ºC in the dark. The following fluorophore-conjugated rat anti-mouse antibodies (Biolegend, London, UK) were used for analysis of mouse EVs and cells: CD11b (M1/70) PE, Ly6C (HK1.4) PE-Cy7, Ly6G (1A8) APC, TER-119 (TER-119) PE, CD31 (MEC 13.3) PE or PE-Dazzle™ 594, CD41 (MWReg30) PE-Cy7, CD45 (30-F11) PerCP or PE-Cy7, F4/80 (BM8) APC, MHCII (M5/114.15.2) PerCP. The following fluorophore conjugated mouse anti-human antibodies (Biolegend) were used for



AJRCMB Articles in Press. Published September 23, 2022 as 10.1165/rcmb.2022-0207OC

analysis of human experiments: CD66b (G10F5) PE, CD45 (2D1) APC, CD61 (VI-PL2) APC, CD42b (HIP1) PE, CD31 (WM59) PE-Dazzle™ 594, CD146 (P1H12) FITC, CD62E (HAE-1f) PE, CD54 (HA58) PE-Cy5, CD106 (STA) APC, CD14 (HCD14) PE-Cy7, CD45 (2D1) APC-Cy7 and rat anti-mouse/human CD11b (M1/70) PE-Cy7.

Samples were acquired using a Cyan ADP flow cytometer (Beckman Coulter, High Wycombe, UK). For EV detection and quantification, EV containing samples were acquired for 1 min at minimum flow rate using a side scatter trigger threshold, as described previously (4, 12). EVs were distinguished from other particles and instrument noise by three widely accepted characteristics: size ≤1.0 μm, using fluorescent calibration beads (0.88 μm diameter, Sperotech, Lake Forest, IL, USA); expression of classic cell lineage plasma-membrane markers; and sensitivity to Triton X-100 (0.1%). EV counts were determined using Accucheck counting beads (Thermo Fisher Scientific, Paisely, UK) with subtraction of Triton X-100 insensitive events from the total EV marker-positive gated events. Data were analysed with FlowJo software (Three Star, Ashland, OR, USA).

***Bradford assay***

The protein concentrations of BALF samples from animal studies were measured via the Bradford assay (Bio-Rad Laboratories, Watford, UK), with absorbances measured at 595 nm (Biotex ELx800).

***Measurement of soluble inflammatory mediators/markers***

IPL perfusates and cell culture supernatants were thawed and analysed using Duoset sandwich ELISA or Quantikine ELISA kits (R&D Systems, Abingdon, UK) according



AJRCMB Articles in Press. Published September 23, 2022 as 10.1165/rcmb.2022-0207OC

to the manufacturer's instructions were read at 450 nm in an absorbance microplate reader (Biotex ELx800).



AJRCMB Articles in Press. Published September 23, 2022 as 10.1165/rcmb.2022-0207OC

## REFERENCES

1. O'Dea KP, Wilson MR, Dokpesi JO, Wakabayashi K, Tatton L, van Rooijen N, Takata M. Mobilization and margination of bone marrow Gr-1$^{high}$ monocytes during subclinical endotoxemia predisposes the lungs toward acute injury. *Journal of immunology (Baltimore, Md : 1950)* 2009;182(2):1155-1166.

2. Imai T, Takahashi Y, Nishikawa M, Kato K, Morishita M, Yamashita T, Matsumoto A, Charoenviriyakul C, Takakura Y. Macrophage-dependent clearance of systemically administered B16Bl6-derived exosomes from the blood circulation in mice. *J Extracell Vesicles* 2015;4:26238.

3. Matsumoto A, Takahashi Y, Chang HY, Wu YW, Yamamoto A, Ishihama Y, Takakura Y. Blood concentrations of small extracellular vesicles are determined by a balance between abundant secretion and rapid clearance. *J Extracell Vesicles* 2020;9(1):1696517.

4. O'Dea KP, Tan YY, Shah S, B VP, K CT, Wilson MR, Soni S, Takata M. Monocytes mediate homing of circulating microvesicles to the pulmonary vasculature during low-grade systemic inflammation. *J Extracell Vesicles* 2020;9(1):1706708.

5. Tacke F, Ginhoux F, Jakubzick C, van Rooijen N, Merad M, Randolph GJ. Immature monocytes acquire antigens from other cells in the bone marrow and present them to t cells after maturing in the periphery. *J Exp Med* 2006;203(3):583-597.

6. Sunderkotter C, Nikolic T, Dillon MJ, Van Rooijen N, Stehling M, Drevets DA, Leenen PJ. Subpopulations of mouse blood monocytes differ in maturation stage and inflammatory response. *Journal of immunology (Baltimore, Md : 1950)* 2004;172(7):4410-4417.



AJRCMB Articles in Press. Published September 23, 2022 as 10.1165/rcmb.2022-0207OC

7. van Rooijen N, Kors N, Kraal G. Macrophage subset repopulation in the spleen: Differential kinetics after liposome-mediated elimination. *J Leukoc Biol* 1989;45(2):97-104.

8. Yamaguchi K, Yu Z, Kumamoto H, Sugawara Y, Kawamura H, Takada H, Yokochi T, Sugawara S, Endo Y. Involvement of kupffer cells in lipopolysaccharide-induced rapid accumulation of platelets in the liver and the ensuing anaphylaxis-like shock in mice. *Biochim Biophys Acta* 2006;1762(3):269-275.

9. Tatham KC, O'Dea KP, Romano R, Donaldson HE, Wakabayashi K, Patel BV, Thakuria L, Simon AR, Sarathchandra P, Harefield Pi, et al. Intravascular donor monocytes play a central role in lung transplant ischaemia-reperfusion injury. *Thorax* 2018;73(4):350-360.

10. English D, Andersen BR. Single-step separation of red blood cells. Granulocytes and mononuclear leukocytes on discontinuous density gradients of Ficoll-Hypaque. *Journal of immunological methods* 1974;5(3):249-252.

11. Wakabayashi K, Wilson MR, Tatham KC, O'Dea KP, Takata M. Volutrauma, but not atelectrauma, induces systemic cytokine production by lung-marginated monocytes. *Crit Care Med* 2014;42(1):e49-57.

12. O'Dea KP, Porter JR, Tirlapur N, Katbeh U, Singh S, Handy JM, Takata M. Circulating microvesicles are elevated acutely following major burns injury and associated with clinical severity. *PLoS One* 2016;11(12):e0167801.



AJRCMB Articles in Press. Published September 23, 2022 as 10.1165/rcmb.2022-0207OC

**Supplementary Figure E1**

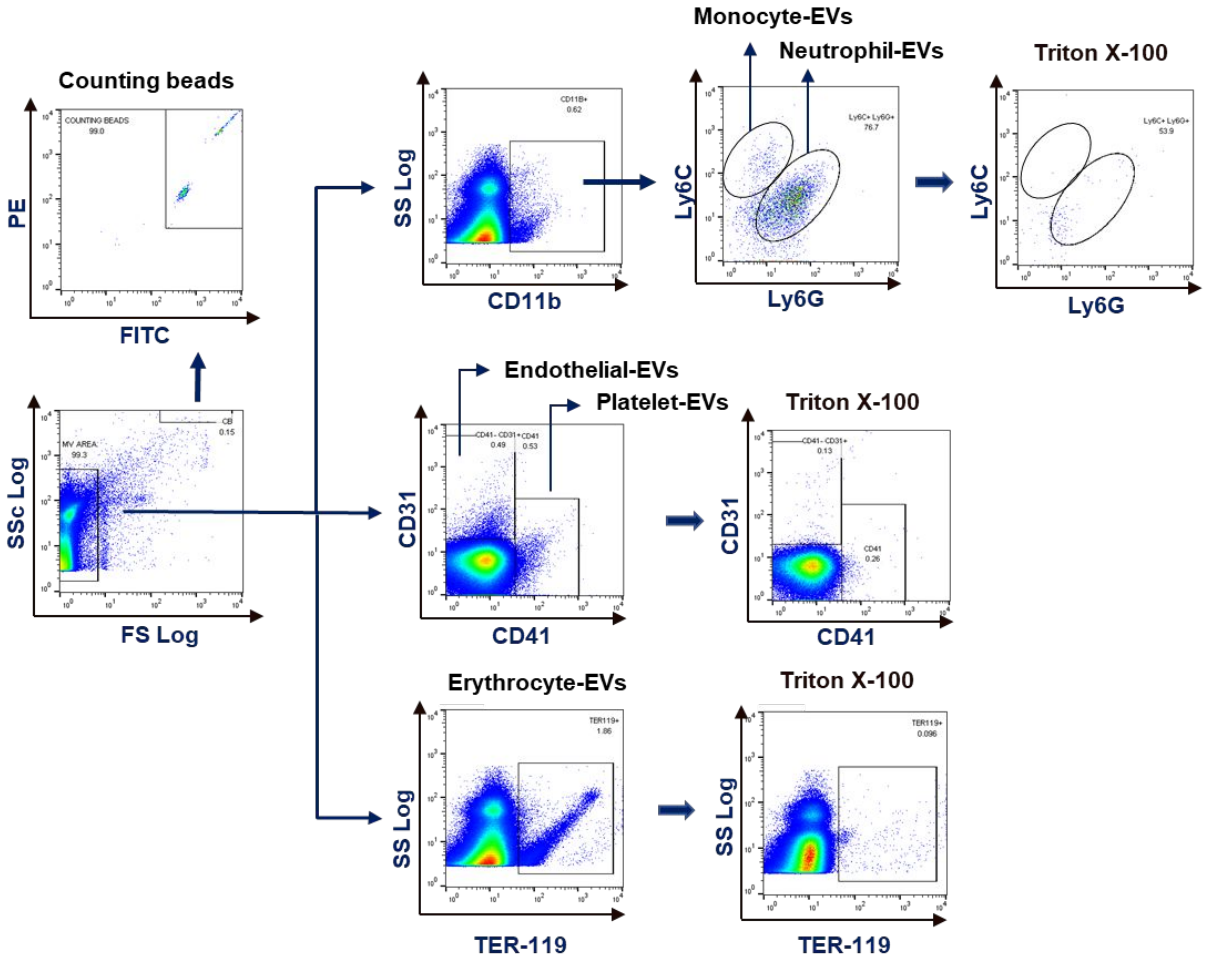


**Figure E1. Analysis of circulating EV subtypes in mice by flow cytometry.** EVs were analyzed in platelet-poor plasma from LPS treated (2 µg, i.v., 1 h) mice by flow cytometry. Gating of EVs was based on a forward scatter size (FS) threshold set using fluorescent sizing calibration beads (0.88 µm, Sperotech) as described previously (1). Myeloid-EVs were identified as CD11b+ events, and their main subpopulations were identified as CD11b+, Ly6C+, Ly6G+ neutrophil-EVs and CD11b+, Ly6C+, Ly6G-, Ly6C$^{high}$ monocyte-EVs. Platelet-EVs were identified as CD41+, endothelial-EVs as CD31+, CD41- and erythrocyte-EVs as TER-119+. EV counts were determined using counting beads (Accucheck counting beads, Thermo Fisher Scientific, UK) following subtraction of Triton X-100 insensitive events.

AJRCMB Articles in Press. Published September 23, 2022 as 10.1165/rcmb.2022-0207OC

**Supplementary Figure E2**

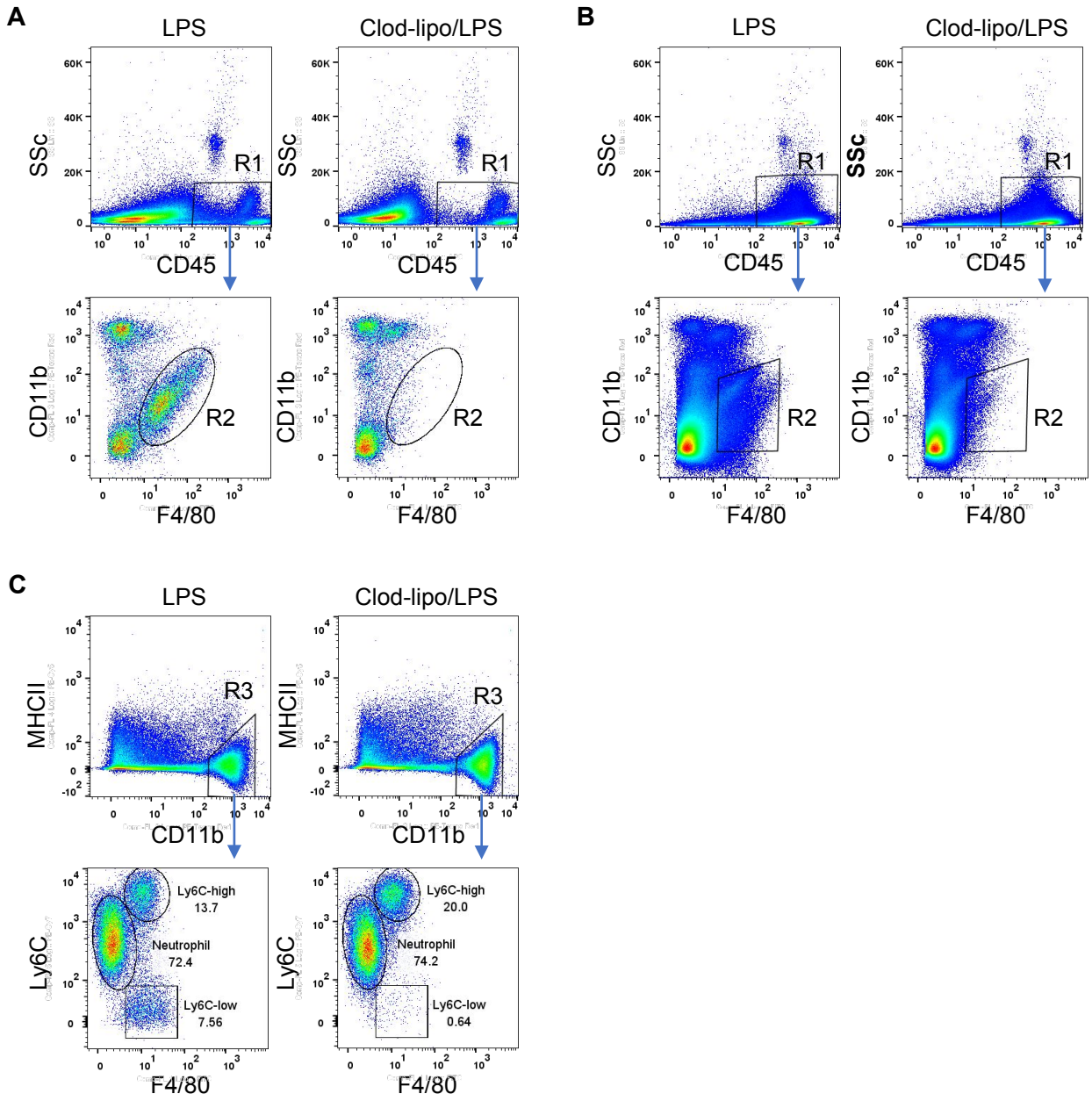


**Figure E2. Assessment of macrophage and monocyte depletion by i.v. clodronate-liposome injection (–48 h)**. Mice were injected i.v. (via tail vein) with 0.2 ml of clodronate-liposome (clod-lipo) suspension. After 48 h, mice were challenged with LPS (i.v., 2 μg in 0.2 ml PBS) to generate of circulating EVs for adoptive transfer. At 1 h post-LPS injection, blood was collected by cardiac puncture and single cell suspensions were prepared from liver (**A**), spleen (**B**) and lung (**C**) tissue for evaluation of macrophage and monocyte levels by flow

AJRCMB Articles in Press. Published September 23, 2022 as 10.1165/rcmb.2022-0207OC

cytometry, as described previously (1). In liver and spleen cell suspensions, leukocytes were identified as CD45-positive events (**R1**) and resident macrophages as F4/80-positive and CD11b low-medium events (**R2**). In lungs, intravascular myeloid cells were identified as CD11b-positive, MHCII-negative (**R3**), as described previously (2). Monocyte Ly6$^{high}$ and Ly6C$^{low}$ subsets were distinguished from neutrophils based on their expression of F4/80; percentage values are shown for each gated population. Clodronate-liposome treatment resulted in relative reductions of macrophage populations in the liver and spleen, and Ly6C$^{low}$ monocytes in the lungs. Levels of Ly6C$^{high}$ monocytes were not reduced due to their repopulation from the bone marrow pool at 48 h post clodronate-liposome treatment (3). Alveolar macrophages are not depleted by this route of clodronate-liposome injection (not shown).

AJRCMB Articles in Press. Published September 23, 2022 as 10.1165/rcmb.2022-0207OC

**Supplementary Figure E3**

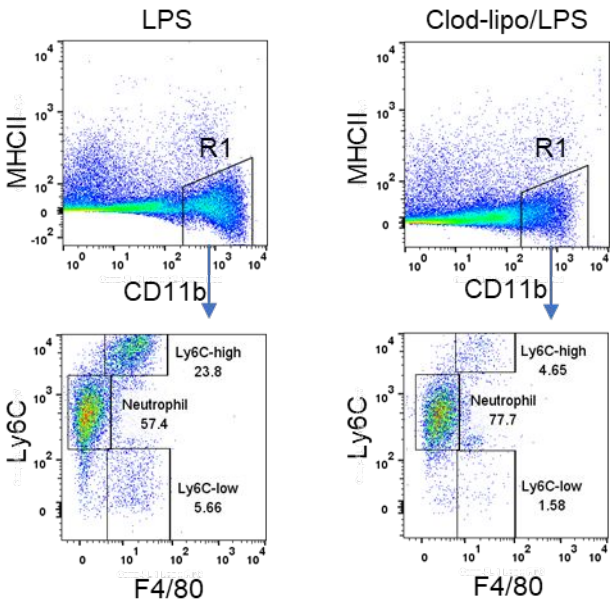


**Figure E3. Assessment of lung-marginated monocyte depletion by i.v. clodronate-liposome injection (–24 h).** Mice were injected i.v. (via tail vein) with 0.2 ml of clodronate-liposome (clod-lipo) suspension. After 24 h, mice were challenged with LPS (i.v., 20 ng in 0.2 ml PBS) 2 h prior to IPL setup. Following 2 h recirculating perfusion of the lungs (without EV infusion), a single cell suspension was prepared from the left lung. Intravascular myeloid cells were identified as CD11b-positive, MHCII-negative (**R1**) (2). Clodronate-liposome treatment resulted in relative reductions in both $Ly6C^{high}$ and $Ly6C^{low}$ monocytes, as described previously (3).

AJRCMB Articles in Press. Published September 23, 2022 as 10.1165/rcmb.2022-0207OC

**Supplementary Figure E4**

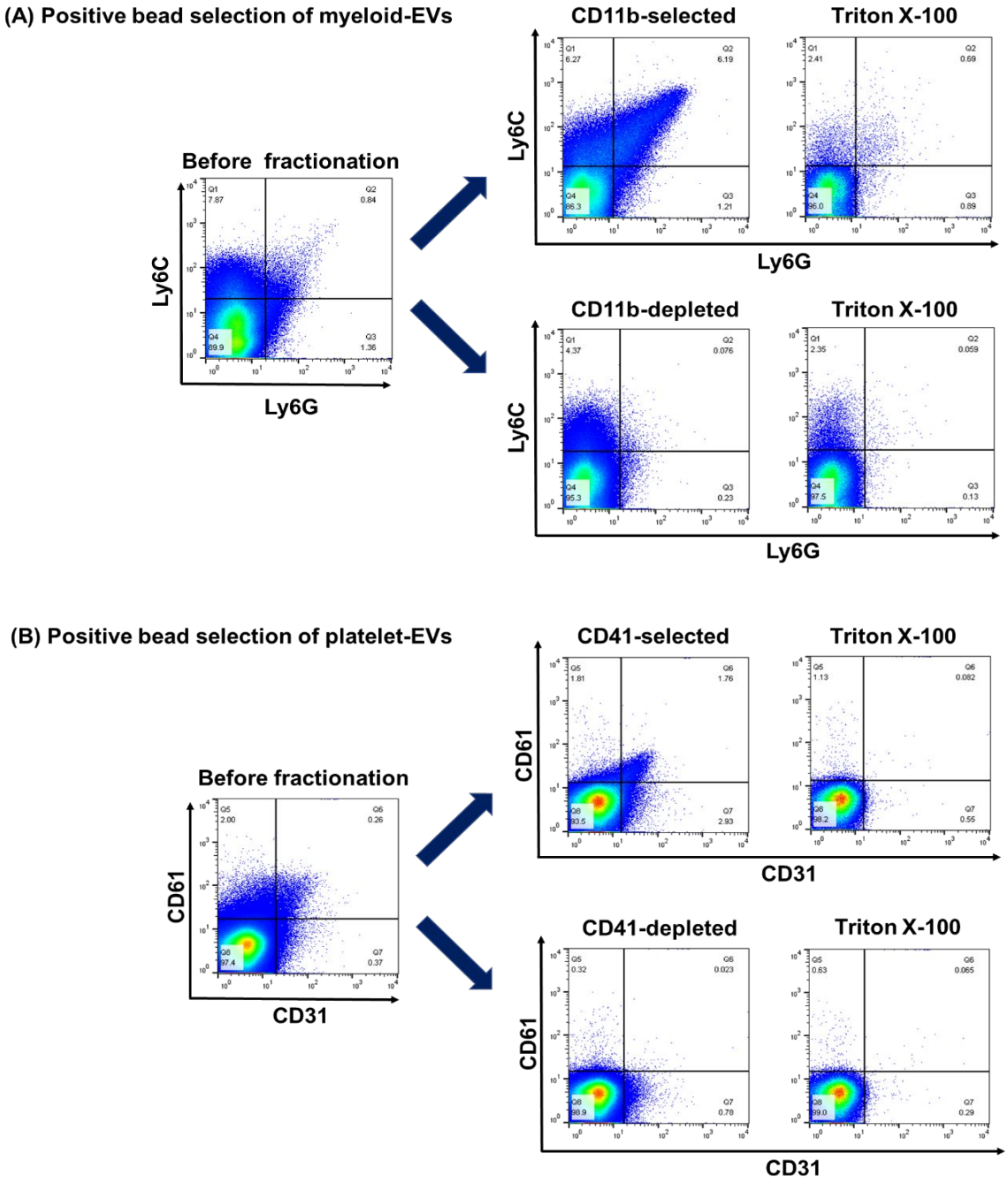


**Figure E4. Immunoaffinity isolation of mouse circulating CD11b+ (myeloid) and CD41+ (platelet) EV subtypes.** Platelet-poor plasma from clodronate-liposome pre-treated endotoxemic mice was centrifuged at 20,800 × *g* for 30 mins to sediment EVs. EVs were resuspended in PBS-BSA and incubated with anti-CD11b MACS® MicroBeads ( ≤0.05 μm

AJRCMB Articles in Press. Published September 23, 2022 as 10.1165/rcmb.2022-0207OC

diameter, Miltenyi Biotec, Bisley, UK) for myeloid EV isolation (**A**), or an anti-CD41 biotin antibody, followed by anti-biotin MACS® MicroBeads for platelet-EV isolation (**B**). The EV-bead suspension was then passed through a magnetized LS column. After three-column washes with 3 ml of PBS-BSA, the bound fraction was eluted and washed. EVs in the eluted fractions were analysed using complementary surface markers: Ly6C/Ly6G for CD11b-selected EVs and CD61/CD31 for CD41-selected EVs. For each separation, the column bound ('selected') and flow-through unbound fractions ('depleted') fractions are shown to demonstrate the effective separation of target EVs from total EVs. A distinct but unknown CD11b-, Ly6C+, Ly6G- population was found consistently in the CD11b-bead unbound fraction.

AJRCMB Articles in Press. Published September 23, 2022 as 10.1165/rcmb.2022-0207OC

**Supplementary Figure E5**

**A. EV donor mouse**

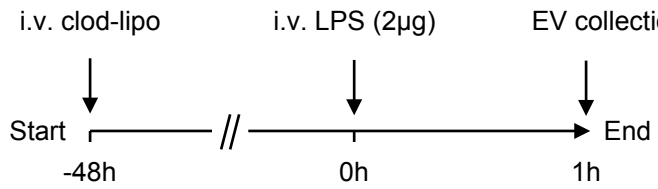


**B. IPL recipient mouse**

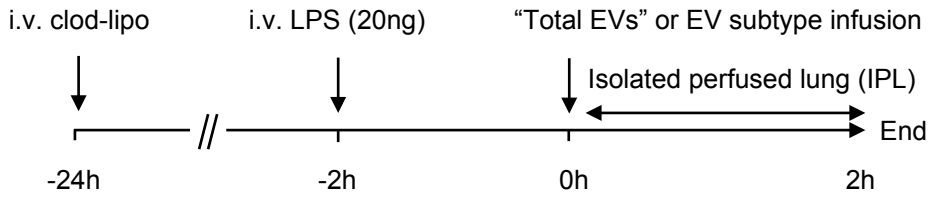


**Figure E5. Experimental design of adoptive transfer of *in vivo* EVs to *ex vivo* IPL. (A)** EV donor mice were treated with clodronate-liposomes (i.v., 0.2 ml) 48 h before LPS challenge (i.v., 2 µg). At 1 h post-LPS, mice were euthanized to obtain circulating EVs, with/without subsequent immunoaffinity-isolation of EV subtypes. **(B)** IPL recipient mice were treated with/without clodronate-liposomes (i.v., 200 0.2 ml) 24 h prior to LPS challenge (i.v., 20 ng) to deplete intravascular monocytes. At 2 h post-LPS, animals were anesthetized and lungs were isolated and perfused with donor EVs. For "total EVs" treatment, EVs obtained from one donor mouse (~1 × $10^8$) were adoptively transferred into one recipient IPL. For immunoaffinity isolated EV subtype treatments, EVs were isolated from two donor mice and a standardized EV dose of 9 × $10^7$ adoptively transferred into one recipient IPL.

AJRCMB Articles in Press. Published September 23, 2022 as 10.1165/rcmb.2022-0207OC

## Supplementary Figure E6

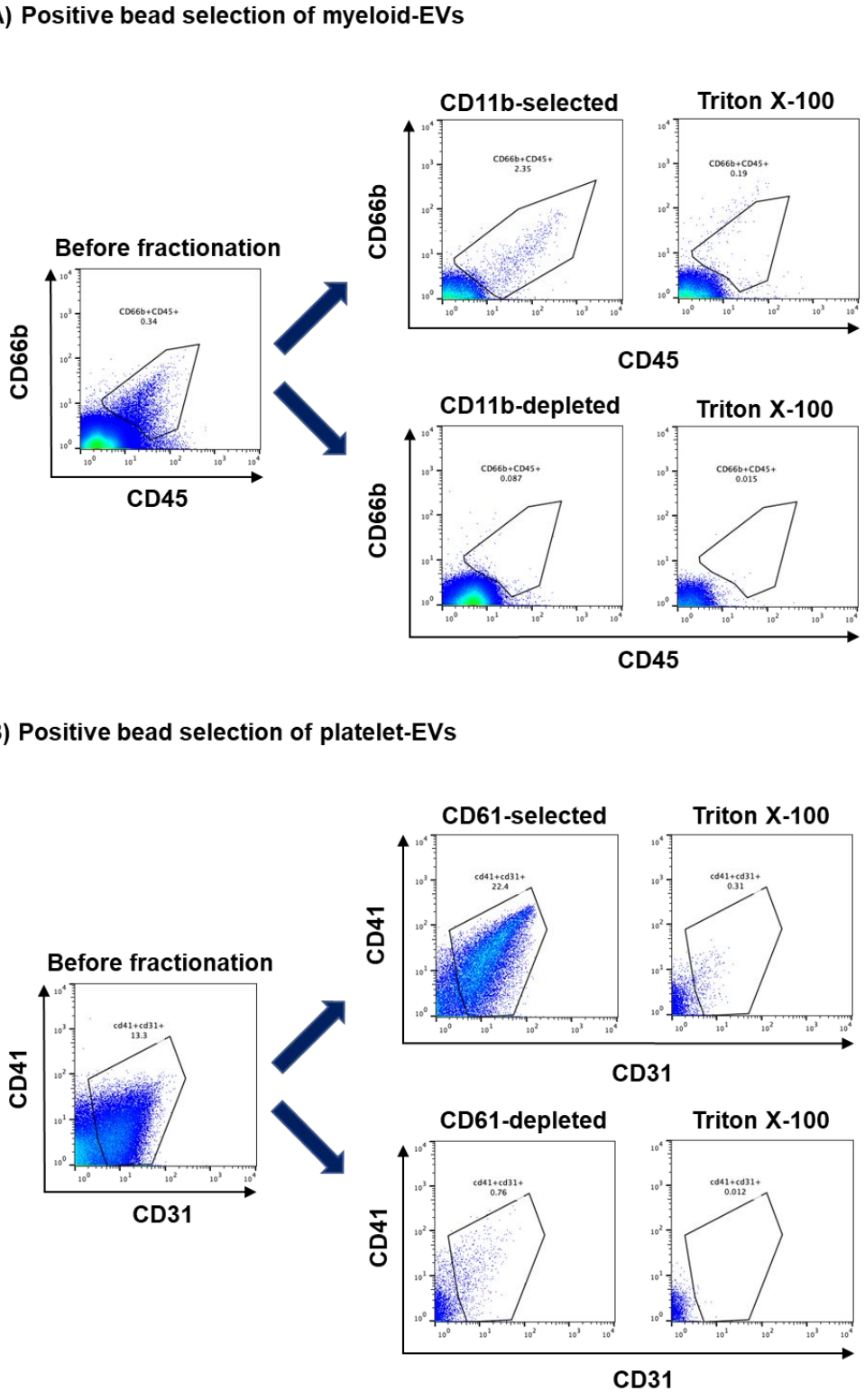


**Figure E6. Immunoaffinity isolation of human blood CD11b+ (myeloid) and CD61+ (platelet) EVs.** Platelet-poor plasma from ex vivo LPS stimulated human blood was

AJRCMB Articles in Press. Published September 23, 2022 as 10.1165/rcmb.2022-0207OC

centrifuged at 20,800 × *g* for 30 mins to sediment EVs. EVs were resuspended in PBS-BSA and incubated with anti-CD11b MACS® MicroBeads for myeloid EV isolation (**A**), or anti-CD61 MACS® MicroBeads for platelet EV isolation (**B**). The EV-bead suspension was then passed through a magnetized LS column. After three-column washes with 3 ml of PBS-BSA, the bound fraction was eluted and washed. EVs in the eluted fractions were analysed using complementary surface markers: CD66b/CD45 for CD11b-selected EVs and CD41/CD31 for CD61-selected EVs. For each separation, the column bound ('selected') and flow-through unbound fractions ('depleted') fractions are shown to demonstrate the successful separation of target EVs from total EVs.

AJRCMB Articles in Press. Published September 23, 2022 as 10.1165/rcmb.2022-0207OC

**Supplementary Figure E7**

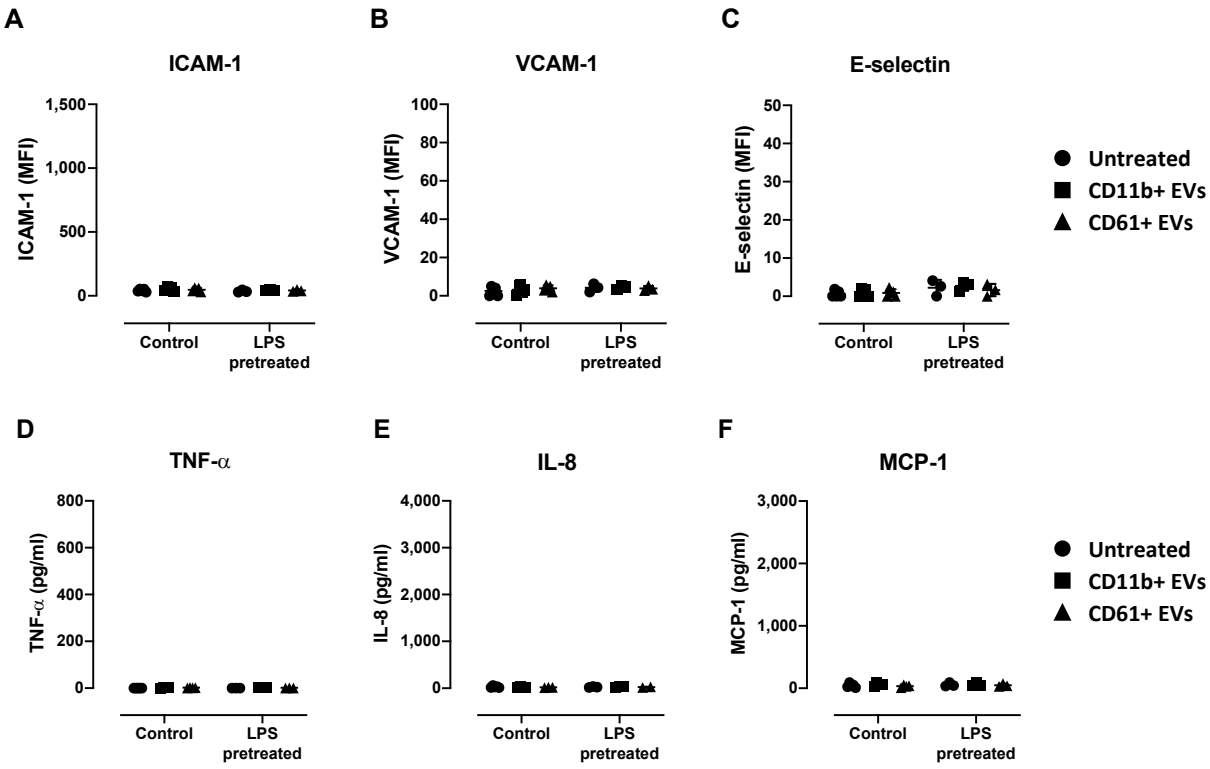


**Figure E7. Treatment of HLMEC monocultures with isolated human EV subtypes.** CD11b+ myeloid- and CD61+ platelet-EVs were isolated by immunoaffinity selection from healthy volunteer blood stimulated with LPS (100 ng/ml) for 3 h. Washed EVs (6
then incubated with HLMEC cultures for 4 h. Under these conditions, EV subtypes produced neither endothelial cell activation nor pro-inflammatory cytokine release. (Mean ± SD, n=3-5)

AJRCMB Articles in Press. Published September 23, 2022 as 10.1165/rcmb.2022-0207OC

## Supplementary Figure E8

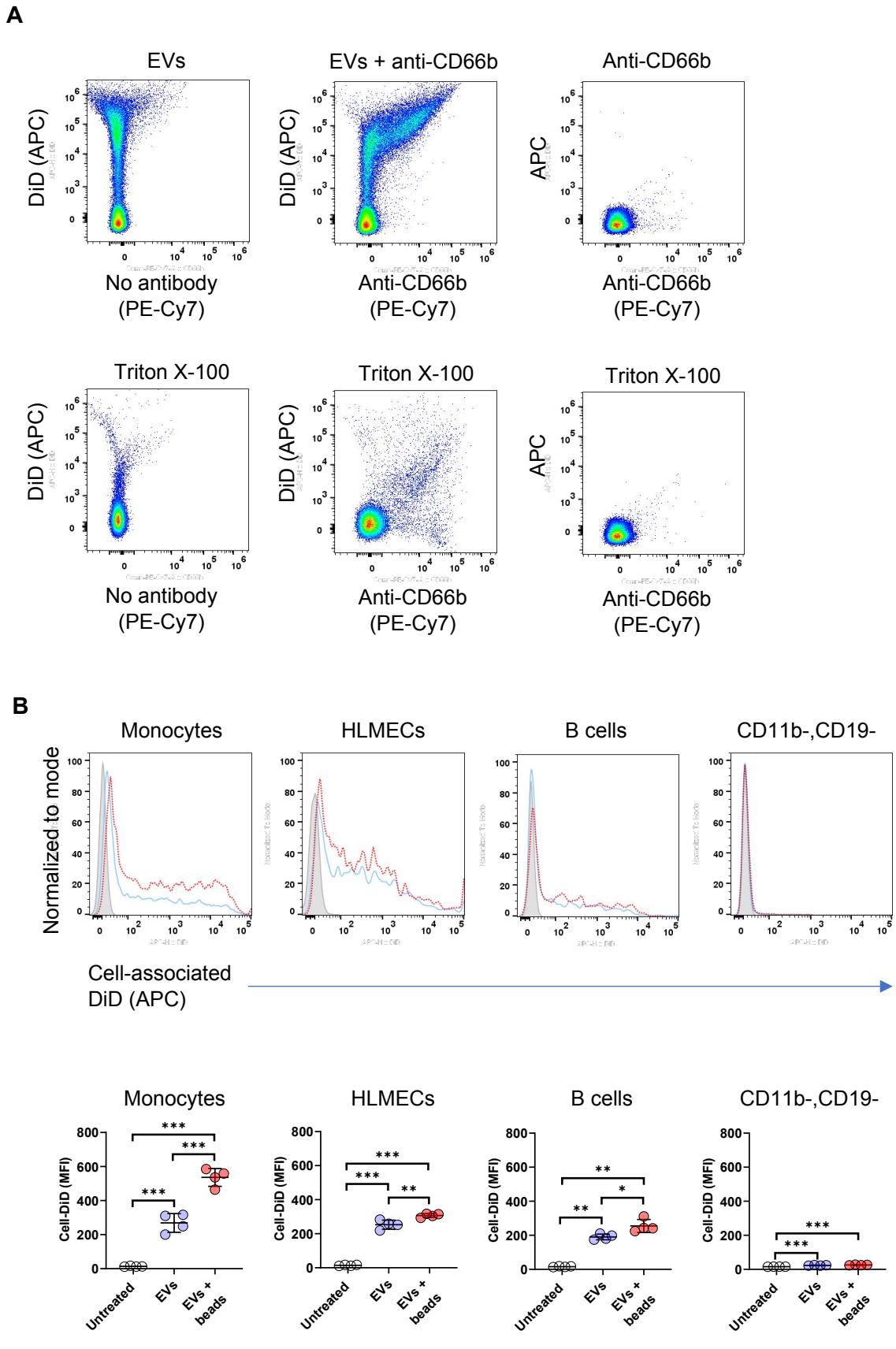

**Supplementary Figure E8. Generation of DiD-labeled EVs released from isolated neutrophils and their uptake in PBMC-HLMEC coculture.** Neutrophils were isolated from healthy volunteer blood and labeled with DiD. After washing to remove unincorporated DiD, cells were stimulated with fMLP (1 μM) for 30 min to produce EVs. (**A**) Flow cytometric analysis indicated the presence of both CD66b+ and CD66b- DiD-labelled events (top row). Treatment with Triton X-100 removed the majority of DiD-labelled events indicating detergent sensitivity (bottom row). The CD66b- events were negative for tetraspanins CD9, CD63 and CD81 suggesting they were not exosomes (data not shown). (**B**) Histogram overlays showing DiD fluorescence associated with main cell populations in coculture after 1 h incubation with DiD labeled EVs (25,000 fluorescent units/ml). No EVs, gray fill; EVs without anti-CD11b beads, solid blue line; EVs with anti-CD11b beads, red dotted line. (**C**) DiD fluorescence (MFI: mean fluorescence intensity) in each cell population analysed by one-way ANOVA with Bonferroni's correction tests (mean ± SD). n = 4, * $p<0.05$, ** $p < 0.01$, *** $p < 0.001$.

AJRCMB Articles in Press. Published September 23, 2022 as 10.1165/rcmb.2022-0207OC

## REFERENCES

1. O'Dea KP, Tan YY, Shah S, B VP, K CT, Wilson MR, Soni S, Takata M. Monocytes mediate homing of circulating microvesicles to the pulmonary vasculature during low-grade systemic inflammation. *J Extracell Vesicles* 2020;9(1):1706708.

2. Patel BV, Tatham KC, Wilson MR, O'Dea KP, Takata M. In vivo compartmental analysis of leukocytes in mouse lungs. *Am J Physiol Lung Cell Mol Physiol* 2015;309(7):L639-652.

3. O'Dea KP, Wilson MR, Dokpesi JO, Wakabayashi K, Tatton L, van Rooijen N, Takata M. Mobilization and margination of bone marrow Gr-1$^{high}$ monocytes during subclinical endotoxemia predisposes the lungs toward acute injury. *Journal of immunology (Baltimore, Md : 1950)* 2009;182(2):1155-1166.

AJRCMB Articles in Press. Published September 23, 2022 as 10.1165/rcmb.2022-0207OC